



## Quantitative evaluation of *n*-alkanes, PAHs, and petroleum biomarker accumulation in beach-stranded tar balls and coastal surface sediments in the Bushehr Province, Persian Gulf (Iran)



Mehdi Dashtbozorg<sup>a</sup>, Alireza Riyahi Bakhtiari<sup>b,\*</sup>, Mohammad Reza Shushizadeh<sup>c</sup>, Lobat Taghavi<sup>a</sup>

<sup>a</sup> Department of Environmental Science, Faculty of Natural Resources and Environment, Science and Research Branch, Islamic Azad University, Tehran, Iran

<sup>b</sup> Department of Environmental Sciences, Faculty of Natural Resources and Marine Sciences, Tarbiat Modares University, Noor, Mazandaran, Iran

<sup>c</sup> Marine Pharmaceutical Science Research Center and Department of Medicinal Chemistry, Ahvaz Jundishapour University of Medical Science, Ahvaz, Iran

### ARTICLE INFO

#### Keywords:

Coastal sediment  
Tar ball  
Petroleum biomarkers  
Source apportionment  
Bushehr Province

### ABSTRACT

Coastal areas within the Bushehr Province (BP), Persian Gulf, Iran, face great challenges due to the heavy organic contamination caused by rapid industrialization, and the presence of numerous oil fields. In addition, in 2014, a significant number of tar balls are found along the coasts of BP. A total of 96 samples (48 coastal sediments and 48 tar balls) were taken from eight sampling points at the BP coast during the summer of 2014. These samples were analyzed to identify the sources and characteristics of their organic matter using diagnostic ratios and fingerprint analysis based on the distribution of the source-specific biomarkers of *n*-alkanes, PAHs,<sup>1</sup> hopanes and steranes. Mean concentration of *n*-alkanes ( $\mu\text{g g}^{-1}$  dw) and PAHs ( $\text{ng g}^{-1}$  dw) varied respectively from 405 to 220,626, and 267 to 23,568 in coastal sediments, while ranged respectively from 664 to 145,285 and 390 to 46,426 in tar balls. In addition, mean concentration of hopanes and steranes ( $\text{ng g}^{-1}$  dw) were between 18.17 and 3349 and 184.66 to 1578 in coastal sediments, whereas in tar balls were 235–1899 and 520–1504, respectively. Pri/Phy<sup>2</sup> ratio was 0.25 to 1.51 (0.65) and 0.36 to 1 (0.63) in coastal sediment and tar ball samples, respectively, and the occurrence of UCM<sup>3</sup> in both matrices, reflecting the petrogenic OM<sup>4</sup> inputs and chronic oil contamination, respectively. The C<sub>30</sub> and C<sub>29</sub> homologues followed Gammacerane were detected in both matrices, in particular those collected from intensive industrial activities, suggesting petrogenic sources of OM. The coastal sediment PAHs profiles were significantly dominated by HMW<sup>5</sup>-PAHs in the Bahregan Beach (BAB) (78% of total PAHs), Bandare-Genaveh (GP) (66%), and Bandare-Bushehr (BUB) (61%) stations, while the Bashi Beach (BSB) (40%), Bandare-Kangan (KP) (57%), and Bandare-Asaluyeh (AP) (51%) stations exhibited higher proportion of LMW<sup>6</sup>-PAHs. PCA<sup>7</sup> indicated that the tar ball and coastal sediment samples deposited along the Southwest of the BP beaches are most likely originated from the Abuzar oil. Based on the intensity of the anthropogenic activities, NPMDS<sup>8</sup> analysis revealed that the GP, BAB, NNP, AP, and KP sampling sites had a high concentration of detected organic pollutants. To the best of our knowledge, this is the first study that investigates oil pollution in coastal sediments and tar balls in the BP, providing insights in to the fate of oil in the coastal areas of the Persian Gulf, Iran.

\* Corresponding author. Department of Environmental Sciences, Faculty of Natural Resources and Marine Sciences, Tarbiat Modares University, Noor, Mazandaran, Iran

E-mail address: [Riahi@modares.ac.ir](mailto:Riahi@modares.ac.ir) (A. Riyahi Bakhtiari).

<sup>1</sup> Polycyclic Aromatic Hydrocarbons

<sup>2</sup> Pristane/Phytane

<sup>3</sup> Unresolved Complex Mixture

<sup>4</sup> Organic Matter

<sup>5</sup> Higher Molecular Weight

<sup>6</sup> Lower Molecular Weight

<sup>7</sup> Principal Component Analysis

<sup>8</sup> Non-Parametric Multi-Dimensional Scaling

## 1. Introduction

In recent years, significant marine and coastal environmental pollution, particularly oil pollutants from sources near the shore, have affected coastal ecosystems (Singkran, 2013), resulting in research on the critical impacts of this pollution on marine habitats, fisheries, wildlife, and human activities (Santos et al., 2013; Mokhtari et al., 2015; de Andrade Passos et al., 2010; Lamine and Xiong, 2013). Marine and coastal sediments provide valuable information on past or on-going environmental variables, including natural and human-induced activities (Ranjbar Jafarabadi et al., 2017a, 2017b, 2017c, 2018a, 2018b; 2019b; Shirneshan et al., 2016; Jeng, 2007). Human activities, such as expanding industrialization and urbanization, which have led to oil and gas exploration, have resulted in the disbursement of oil and gas related substances from oil wells in to marine environments (Ramsey et al., 2014; Islam and Tanaka, 2004; Vaughan et al., 2019).

Environmental pollution has been assessed using organic markers (Ranjbar Jafarabadi et al., 2017a). Geochemical organic markers have been broadly applied to distinguish the organic matter (OM) in various environments and on various timescales and may be assigned to certain sources (Takada and Eganhouse, 1998; Derrien et al., 2017; Cabral et al., 2018). These molecules are identified using comparatively high chemical stability to degradation processes, their constant molecular structure, and their direct association with anthropogenic (oil and by-products) and/or biogenic (marine and terrestrial) organic matter (Colombo et al., 2005; Volkman, 2005).

Petroleum compounds consist of a complex mixture of aliphatic, polycyclic aromatic hydrocarbons, and non-hydrocarbons (Bayona et al., 2015). Geochemical markers, such as *n*-alkanes, PAHs, hopanes, and steranes, may be used to explain the origin of the hydrocarbons deposited in a specific marine system and confirm the contribution of petroleum products (Peters et al., 2005). These geochemical markers are able to distinguish between oils to determine their sources, original depositional environment, maturation, and level of biodegradation (Peters and Moldowan, 1993). Among petroleum hydrocarbons, *n*-alkanes and polycyclic aromatic hydrocarbons (PAHs) are extensively applied to identify the origin of organic matter from biogenic, petroleum/oil and its by-products, and combustion residues in various environmental matrices (Gao et al., 2007; Liu et al., 2014; Martins et al., 2015; Dudhagara et al., 2016; Ranjbar Jafarabadi et al., 2017a, 2018a, 2019a; He et al., 2018; Aghadadashi et al., 2016; Shirneshan et al., 2017). Although *n*-alkanes mainly have petroleum origin in the environment (petroleum and fossil fuels) (Volkman et al., 1992; Vaezzadeh et al., 2017), nonetheless, they are synthesized by marine (phytoplankton and zooplankton) and terrestrial organisms, higher plants, and bacteria (Cripps, 1989; Wang et al., 2009).

PAHs are pollutants associated mostly with anthropogenic sources, such as incomplete combustion of fossil fuels, coal, and biomass and crude petroleum/oil and its refined by-products (Guitart et al., 2007; Liu et al., 2009). PAHs have become a great concern due to their persistence, high toxicity, mutagenicity, carcinogenicity, and the hazards they pose to human health and the environment (Wu et al., 2014). Another semi-volatile organic compounds are hopanes (penta-cyclic triterpene) and steranes which can be totally utilized as molecular markers for petroleum pollution as they are resistant to degradation, semi-volatile and present in discrepant quantities in high boiling point products of petroleum in various origins and maturity (Peters et al., 2005; Kao et al., 2015; Huang et al., 2014; Vaezzadeh et al., 2017). Although they are common constituents of crude oil, they are also originating from the cell membrane of prokaryotes in marine ecosystem (Manan et al., 2011; Huang et al., 2014; Vaezzadeh et al., 2017). In addition, the presence of hopanes and steranes in environmental samples exhibits pollution from fossil fuel residues (Medeiros et al., 2005).

The residual oil mixtures interact with suspended solids in the coastal waters and sinks to the sandy bottom to create immobile submerged oil mats (consist of 70% to 95% sand) and mobile surface

residual balls (tar balls, distributed on the shores) (Hayworth et al., 2011; OSAT-2, 2011; OSAT-3, 2013; Michel et al., 2013; Bacosa et al., 2016). Tar balls are formed from tanker accidents, oil well blow-outs, natural submarine seepages, discharge of ballast water and tanker-wash occur (Kvenvolden et al., 2000; Hostettler et al., 2004; Bacosa et al., 2016). Tar balls are consisting of various mixtures of hydrocarbon such as *n*-alkanes, Isoprenoids, polycyclic aromatic hydrocarbons (PAHs), hopanes, and steranes (Shirneshan et al., 2016; Butler et al., 1998) which are toxic to marine life causing damage to algae and phytoplanktons which constitute majority of primary producers in marine food chain (Nkem et al., 2016; Dietrich et al., 2014). These pollutants enter the food chain, accumulate in tissues of living organisms and cause carcinogenic damages (Perelo, 2010; Hassanshahian et al., 2014) and eventually could pollute coastal surface sediments. Furthermore, surface sediment in the Persian Gulf contains considerable levels of petroleum biomarkers (Ranjbar Jafarabadi et al., 2017a, 2018b), so that, surface sediments and tar balls could pose long-term environmental risk to the marine ecosystem (Suneel et al., 2014; Warnock et al., 2015; Yin et al., 2015; Ranjbar Jafarabadi et al., 2017c, 2018a; Dauner et al., 2018).

The Persian Gulf has about 60% of the world's proven oil reserves and is visited by two-thirds of the world's marine petroleum traffic, while it just covers < 0.1% of the marine surface of the world (Khan, 2002). Bushehr province with a long coastline (> 707 km) along the Persian Gulf with its strategic and geopolitical position, as a one of the most important port, is located in southwestern of Iran and northern part of the Persian Gulf (Noroozi Karbasdehi et al., 2017). Due to the high density of oil facilities, the high volume of oil shipment and the semi-closure of the Persian Gulf, the risk of oil pollution in this area has increased significantly and become one of the most anthropogenically impacted regions in the world (Mehdinia et al., 2015; Burton and Johnston, 2010; Vaughan et al., 2019; Burt, 2014). Development has already affected as much as 40% of the coastlines of some Persian Gulf countries (Niamaimandi et al., 2017). However, the Bushehr coast is often under the menace of tar balls, which has become a common phenomenon. During summer of 2014, most of the Bushehr beaches were affected by tar ball deposition. This deposition attracts a huge public concern as the on-going recreational activities on beaches get seriously affected, which in turn affects the tourism industry, and it is becoming an environmental problem. Moreover, the tar ball being a carcinogenic, it affects the marine life and tar ball pollution degrades health of the coastal waters off Bushehr and coastal areas in the Persian Gulf. Hereupon, the monitoring of oil pollutants in a dynamic marine system particularly coastal settings is worth investigating and tracing of the sources of these tar balls is highly essential. To the best of our knowledge, up to now, there has been no investigation on tar balls and coastal sediments in the Bushehr Province and no report can be found that identified the origin of oil pollution in tar balls and sediments of southwest coasts of the Persian Gulf by using biomarkers. Due to the several anthropogenic impacts on this large coastal area in the Persian Gulf, the purposes of this study were 1) to determine the concentrations of oil biomarkers (*n*-alkanes, PAHs, hopane and sterane), in coastal surface sediments and importantly enormous quantities of tar balls landed on the coast of Bushehr Province, 2) to assess the sources of organic matter with diagnostic ratios, 3) to apply the fingerprint techniques of diagnostic ratios of hopanes and steranes biomarkers using principle component analysis (PCA) to identify the sources of tar balls and petroleum hydrocarbons in coastal sediments 4) to provide new information regarding the contamination status of this area.

## 2. Materials and methods

### 2.1. Study area and sampling procedure

The Persian Gulf (E: 48°–57°, N: 24°–30°), which is an extension of the Indian Ocean and a shallow and semi-enclosed basin in a typically

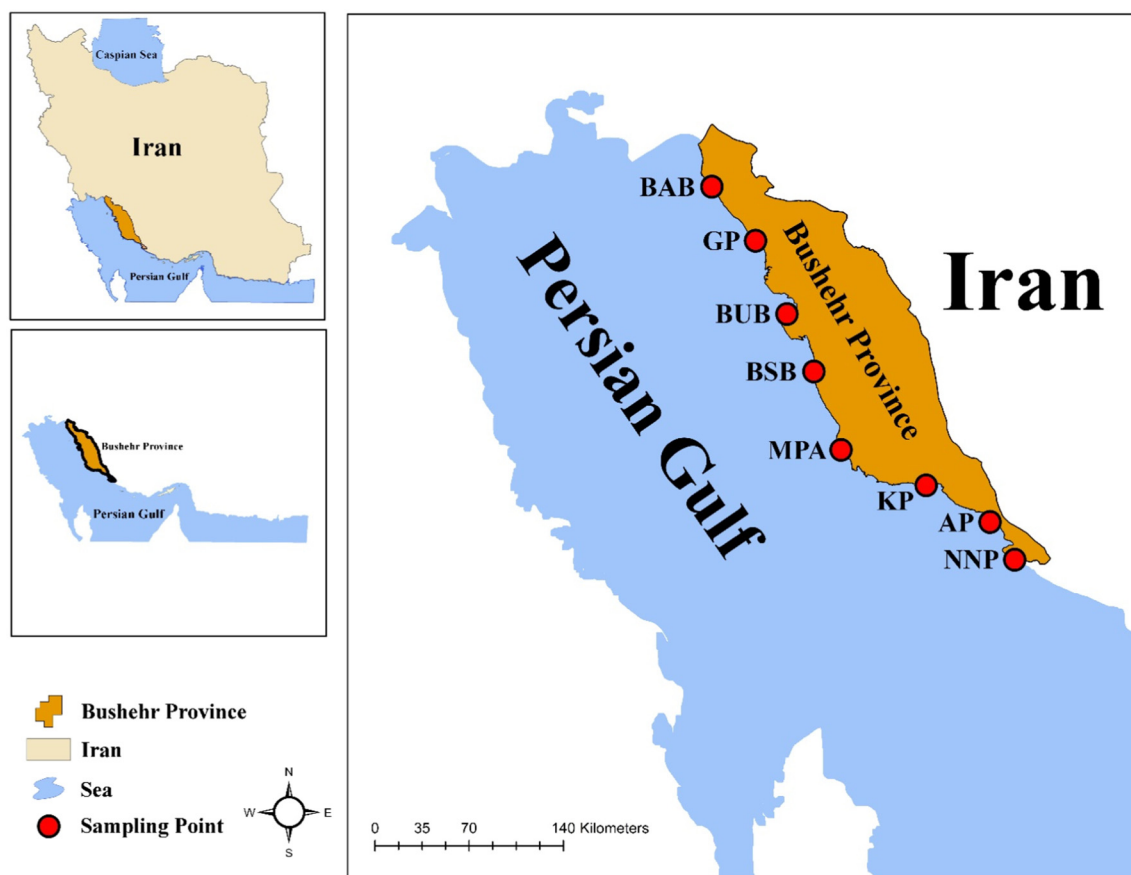


Fig. 1. Location of Bushehr province in the Persian Gulf, and the surface sediment sampling locations.

arid climate, is located between Iran and the Arabian Peninsula (Ranjbar Jafarabadi et al., 2017a, 2017b, 2018b, 2019a). In Iran, there are several provinces that have large coastlines with the Persian Gulf and the Bushehr province has the largest one with this Gulf (Fig. 1). The region under investigation in this research is the coastal area of the Bushehr province, situated in the south west of the Gulf, Iran, with the coastline long > 700 km, in which there are oil facilities including several oil wells for exploitation and extraction, harbors for transportation, oil condensates, oil pipelines, and etc. A total number of 96 (48 coastal surface sediments and 48 tar balls) samples (with 3 replicates at each station) were taken from eight sampling sites including Bahregan Beach (BAB), Bandare-Genaveh (GP), Bandare-Bushehr (BUB), Bashi Beach (BSB), Mond Protected area (MPA), Bandare-Kangan (KP), Bandare-Asaluyeh (AP), and Naiband National Park (NNP) (Fig. 1, Table S1). Coastal sediments were collected (using a Van Veen grab (50 cm × 50 cm) sampler on July 2014) with similar depth (5 cm) to explain the variations in hydrocarbons concentration with the horizontal gradient of the coastal area. By hand using clean plastic gloves, the tar ball samples were collected. In order to consider whether the collected tar balls were floating or sinking in the water column, we took a subsample and dropped into the beaker of sea water with a salinity of 13 psu and temperature of 29 °C (Suneel et al., 2014; Shirmeshan et al., 2016). Based on our observations, all the tar balls were floating at the surface. All samples (sediment and tar ball) were kept in clean aluminum, foil packets in a cool box, transported to the laboratory of Tarbiyat Modares University, Tehran, Iran, and then stored at −20 °C in the refrigerator until further analysis.

## 2.2. Preparation, extraction and fractionation

A freeze dryer apparatus for 72 h under high vacuum (1.030 mbar

and −50 °C) was applied to dry surface sediments. To analyze the grain-size, a laser particle size analyzer (Malvern Mastersizer 300) was used (Ranjbar Jafarabadi et al., 2017a). Freeze-dried and homogenized coastal sediment samples were utilized for the analysis of TOC using Vario EL III CHNS Analyzer. For total organic nitrogen, the method of Ray et al. (2014) was used. Extraction and fractionation of targeted organic pollutants were conducted based on the approach of Zakaria et al. (2000) and Riyahi Bakhtiari et al. (2009) and his method has been explained in numerous references (Ranjbar Jafarabadi et al., 2017a, 2017b, 2018b; Azimi Yancheshmeh et al., 2014; Shirmeshan et al., 2016; Varnosfaderany et al., 2014). This approach is consisting of a two-step silica gel chromatography and gas chromatography–mass spectrometry (GC–MS). Briefly, a 5 g of each freeze-dried sample were purified and fractionated. Since H<sub>2</sub>S (Hydrogen sulfide) and N<sub>2</sub>S (Nitrogen sulfide) are generated by sulfur bacteria in the sediment and also sulfur and sulfur compounds are present in nearly all bottom sediment and soil samples, due to the nonpolar nature of elemental sulfur, it must be removed by activated Cu to get better resolution in the gas chromatogram of GC–MS. Hereupon, a sulfur removal procedure was performed using activated elemental copper in order to avoid sulfur interferences before analysis (more details in supplementary section). A Soxhlet system was accomplished for extraction of lipids applying 85 ml of dichloromethane (DCM), over 12 h. The sample was then decreased in volume to 5 ml by a rotary evaporation system and then transferred onto the top of 5% H<sub>2</sub>O deactivated silica gel column (1 cm i.d., × 9 cm). With 20 ml of DCM/hexane (1:3, v/v), all hydrocarbons (aliphatic hydrocarbons, hopanes and steranes) were eluted and transferred onto the fully activated silica gel column (0.47 cm i.d. × 18 cm) and eventually eluted with 4 ml hexane to get the aliphatic hydrocarbon (AH) and biomarkers (terpanes and steranes). For obtaining PAHs, the PAH fraction was eluted with 14 mL of

dichloromethane/hexane (1:3, v/v). Eventually, the fractions were evaporated to about 1 mL and transferred to a 1.5 mL glass ampoule. Further reduction with nitrogen gas to dryness was carried out. For tar ball samples, the tar balls were freeze-dried for 24 h prior to further analysis. A 20 mg of the tar ball samples were accurately weighed and dissolved in 2 mL of DCM/*n*-hexane (1,3, v/v) with 200  $\mu$ L of PAH surrogate internal standard, SIS (consists of 5 ppm of each of naphthalene-d8, acenaphthene-d10, phenanthrene-d10, chrysene-d12 and perylene-d4). Similar to surface sediments, the solution was purified and fractionated by the approach explained in Zakaria et al. (2000).

### 2.3. Analytical methods

To determine the concentrations of targeted hydrocarbons comprising *n*-alkanes, PAHs, hopanes and steranes, the analytical procedure described by Zakaria et al. (2000) and Riyahi Bakhtiari et al. (2009) were used. These compounds identified and quantified using Agilent 7890A gas chromatograph coupled with Agilent Technologies 5975C quadrupole mass spectrometer. A fused silica capillary DB-5MS column (30 m  $\times$  0.25 mm i.d., 0.25  $\mu$ m film thickness, J&W Scientific, USA). Based on the retention time, each targeted compound was identified. Samples were injected in split less mode (SIM) (1  $\mu$ L) and high purity helium (99.999%) was applied as carrier gas at 1.0 mL/min. Temperature program in analysis of *n*-alkanes: temperature of injection point was set at 310  $^{\circ}$ C, 70  $^{\circ}$ C (1 min) to 310  $^{\circ}$ C (held 10 min) at 30  $^{\circ}$ C/min. The *n*-alkanes were identified with comparison of retention times with those of known standards of *n*-alkanes ranging from *n*-C<sub>14</sub> to *n*-C<sub>33</sub>. In addition, the UCM concentration was semi-quantitatively specified by integrating the total GC area with subtraction of the resolved peaks and applying the average response factor of C<sub>36</sub> *n*-alkane-d10 during the instrumental calibration. For PAHs, the GC oven was programmed to 60  $^{\circ}$ C for 1 min, 10  $^{\circ}$ C/min to 240  $^{\circ}$ C held for 2 min, 10  $^{\circ}$ C/min to 320 held for 10 min. Both full scan and selected ion monitoring (SIM) modes were applied. PAHs were identified by comparing retention time with those of the appropriate authentic standards and published spectra. For biomarkers, the following instrument parameters: initial temperature, 70  $^{\circ}$ C (maintained for initial 1 min) with ramps of 30  $^{\circ}$ C/min to 150  $^{\circ}$ C and then with ramps of 5  $^{\circ}$ C/min to 290  $^{\circ}$ C and held for 10 min. The injector's temperature was 300  $^{\circ}$ C. As analytical standards for biomarkers, we used 17a(H)-22,29,30-trisnorhopane, 17 $\beta$ (H),21 $\beta$ (H)-hopane, diploptene (17 $\beta$ (H),21 $\beta$ (H)-hop-22(29)-ene), and 17 $\alpha$ (H),21 $\beta$ (H)-hopanes. The steranes standard mixtures include 5 $\alpha$ (H)-cholestane, 24-methyl-5 $\alpha$ (H)-holestane, and 24-ethyl-5 $\alpha$ (H)-cholestane. Predeuterated *n*-tetracosane-d50 (*m/z* 66; relative concentration values) which was used as internal standard added to the samples immediately before the GC analyses (Yunker and Macdonald, 2003; Harris et al., 2011). Characteristic ions were analyzed in single ion monitoring (SIM) mode: *m/z* 191 for tri- and tetracyclic terpane and hopane, *m/z* 217 for  $\alpha\alpha\alpha$ -steranes and *m/z* 218 for  $\alpha\beta\beta$ -steranes (Volkman et al., 1992; Peters and Moldowan, 1993). Schematic diagrams for the procedure of sample preparation, temperature programming for GC–MS experiment and also calibration curves are presented in supplementary section.

### 2.4. Quality assurance and quality control (QA&QC)

To avoid contamination and other interference, QA&QC were conducted strictly for each experimental procedure, comprising extraction, separation and instrumental analysis. To expurgate any organic pollutants, organic solvents were distilled in glass before usage and glass wares were rinsed sequentially with methanol, acetone and distilled hexane, respectively, and kept in an oven at 60  $^{\circ}$ C for 2 h (Ranjbar Jafarabadi et al., 2017a). Standard solutions of targeted petroleum hydrocarbons (*n*-alkanes, PAHs, hopanes, and steranes) were purchased from Sigma Chemical Company. All solvents used for sample processing and analyses (dichloromethane, hexane, and methanol) were

chromatographic grade from Merck. In order to validate the method, recovery experiments were conducted prior to sample extraction. Recoveries were calculated by spiking a known concentration of SIS mixture into the sample followed by performing the entire analytical procedure. The Recoveries of individual spiked SIS were > 88% for alkanes and > 91% for hopanes. The recoveries for PAHs, ranging from 85% to 89%, were used for the recovery correction calculations. In addition, a matrix blank (standards added to a cleaned matrix), reagent blank (only solvent), spiked blank (standard added to solvent) and replicate sediment sample were run with each batch of the sediment samples. Analysis of the blanks confirmed that there was no introduced contamination or other interference over the whole experiment. The relative standard deviation was < 3%, indicating good repeatability. For the aliphatic and aromatic hydrocarbons, limits of detection (LOD = 3S/N, S = signal, N = noise) and limit of quantification (LOQ = 10S/N) of the analytical procedure were respectively 0.002–0.11 and 0.005–0.41  $\mu$ g g<sup>-1</sup>, for *n*-alkanes and 0.003–0.24 and 0.006–0.19 ng g<sup>-1</sup> for PAHs. Moreover, LOD and LOQ of the petroleum biomarkers were 0.10–19.26 and 0.37–81.12 ng g<sup>-1</sup>, respectively.

### 2.5. Data analysis

In the current study, results were mostly processed using the statistical platform R3.1.1 for statistical analysis. The biomarker concentrations (*n*-alkanes, PAHs, hopanes and steranes) distribution normality was explored by the Kolmogorov Smirnov test (all *p* < 0.05). The data of the biomarker concentrations were analyzed using Min, Max and Mean. The sums of the total 22 *n*-alkanes, total 30 PAHs, US EPA 16 priority PAHs, Alkyl PAHs and parent PAHs, total 22 hopanes and 12 steranes were defined as  $\Sigma_{25}$ *n*-alkanes,  $\Sigma_{30}$ PAHs,  $\Sigma_{16}$ PAHs,  $\Sigma$ APAHS,  $\Sigma$ PAPAHS,  $\Sigma_{22}$ hopanes, and  $\Sigma_{12}$ steranes, respectively. The Analysis of Variance (ANOVA) and Duncan test were applied to span any significant differences in the biomarker concentration in the surface sediment and tar ball in various sampling sites, separately. Student's *t*-test was used to evaluate significant differences of biomarker concentrations and biomarker related ratios among discrepant groups of samples, and statistical significance was considered when a *p*-value was < 0.05. To explore the significance of variables that elucidate the potential groupings and patterns of the inherent properties of the whole dataset and to investigate patterns and associations of individual biomarker data, principal component analysis (PCA) with varimax normalized rotation was performed (Ranjbar Jafarabadi et al., 2017a; He et al., 2018; Hammer et al., 2001; Kim et al., 2013). To separate sampling points based on concentration of petroleum biomarkers and bulk parameters, Non-parametric multi-dimensional scaling (NPMDS) was conducted (Ranjbar Jafarabadi et al., 2017a). In order to explore the spatial distribution of the total biomarkers in the surface sediments and tar balls, the data were computed by ordinary kriging (OK) equations with the second order stationary hypothesis (Ranjbar Jafarabadi et al., 2017a). Source apportionment of petroleum biomarkers (both anthropogenic and natural sources) were conducted based on reported chemical markers, diagnostic measures and indices from related investigations (Ranjbar Jafarabadi et al., 2017a, 2018a, 2018b; He et al., 2018; Azimi Yancheshmeh et al., 2014; Riyahi Bakhtiari et al., 2010; Riyahi Bakhtiari et al., 2009; Shirmeshan et al., 2016; Varnosfaderany et al., 2014; Hughes et al., 1995). In addition to diagnostic ratios, since PCA is a multivariate statistical procedure that is broadly applied in the interpretation of oil spill fingerprinting (Suneel et al., 2014; Shirmeshan et al., 2016; Ismail et al., 2016), the source identification of the tar ball and coastal surface sediment samples were also carried out by using PCA.

## 3. Results and discussion

Examples of GC chromatograms with main features and hydrocarbons (e.g., *n*-alkanes, PAHs, APAHS, PAPAHS, hopanes, steranes, and

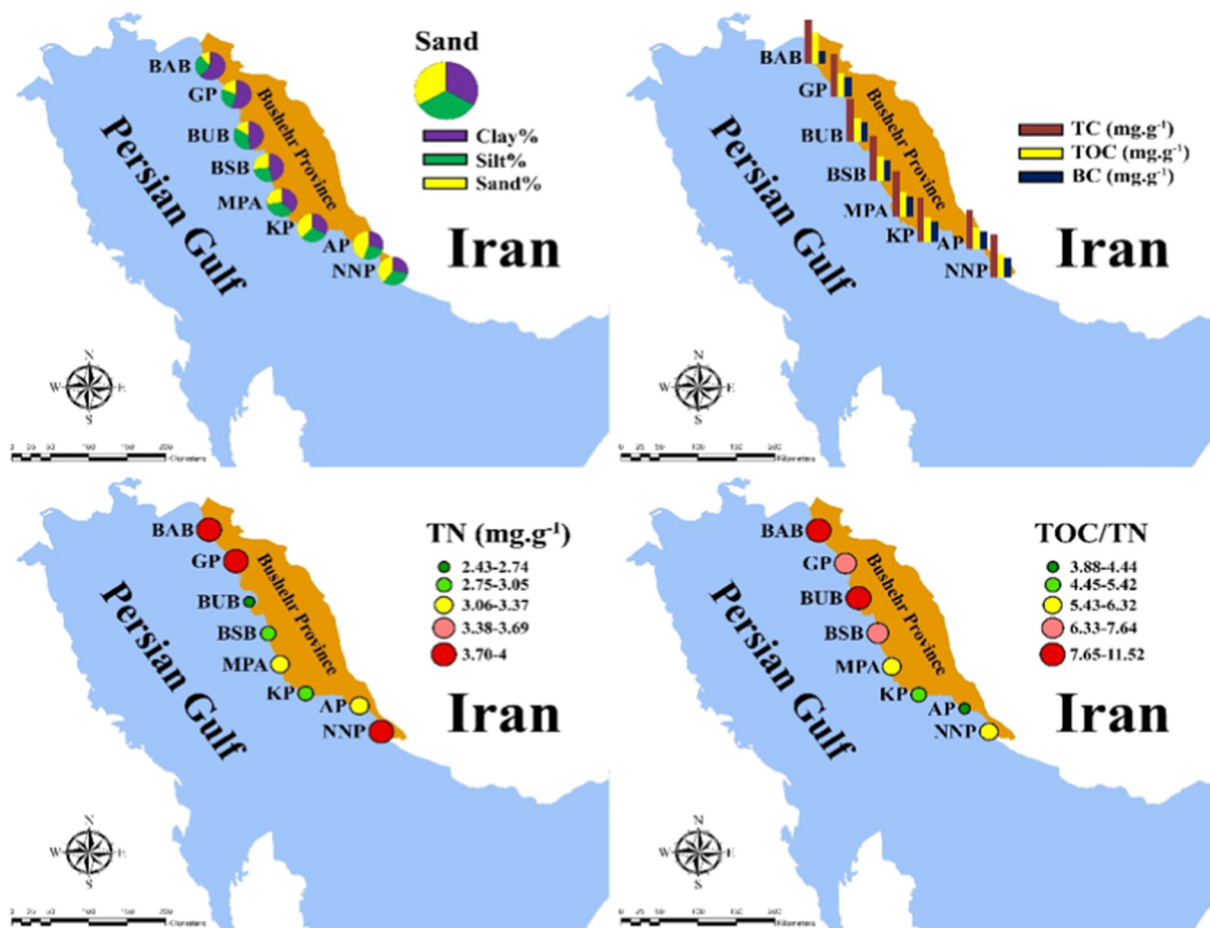


Fig. 2. Spatial variations and distributions of geochemical characterization of the coastal surface sediments including, grain size (a) TC, TOC, BC (b), TN (c), and TOC/TN (d) from sampling sites in the Persian Gulf on July 2014.

UCM) were shown in Fig. S1 and Table S4.

### 3.1. Bulk parameters: Grain size and TOC

The spatial distribution of grain size, TC, TOC, TN, BC and C/N is illustrated in Fig. 2 and Table S3. The coastal surface sediments were predominantly composed of clay (27.1% to 60.5%) and silt (24.5% to 37.2%; Fig. 2), reflecting totally weak to moderate hydrodynamic conditions in the study area. The highest and lowest content clay were observed in BAB (43.2–67%, 61.54%) and NNP (23.1–32%, 27.9%). In addition, the highest sand content was observed at stations AP (43.5–52%, 44.80%) and NNP (24.1–42%, 39.30%), denoting comparatively intense waves and tidal currents close to the coast of these stations, while the lowest content was in BAB (14.2–31.7%, 11.54%), suggesting relatively weak waves and tidal currents near the coast of these stations. One-way ANOVA revealed significant difference in percentage of fine (clay), silt and sand particles among stations ( $p < 0.05$ ). The variation of the clay content in coastal sediments denoted a major positive and negative correlation with silt ( $r^2 > 0.71$ ,  $p < 0.05$ ) and sand ( $r^2 > -0.65$ ,  $p < 0.05$ ), respectively. Generally speaking, spatial trend was observed for clay, silt or sand contents with increasing content of fine and coarse particles toward the north and south west of the study region, respectively. The mean TC (20–67  $\text{mg g}^{-1}$ ), TOC (10–98.44  $\text{mg g}^{-1}$ ) BC (9–25.68  $\text{mg g}^{-1}$ ) contents demonstrated a large range in study region (Fig. 2, Table S3). In addition, there were significant differences ( $p < 0.05$ ) for TC, TOC, and BC among all sampling sites. TC concentrations varied between 20 and 28 (24  $\text{mg g}^{-1}$ ) in AP (in the southwest part of the region) as the lowest concentration and 58–67  $\text{mg g}^{-1}$  (62  $\text{mg g}^{-1}$ ) in BAB (in the

northwestern part of the region) as the highest concentration and were regularly and significantly ( $p < 0.05$ ) augmented from the south toward the north west part of the BP (Fig. 2). Analogously, the highest TOC values ( $\text{mg g}^{-1}$ ) were measured at BAB (42–47, 44), followed by GP (50–57, 52) and BUB (40–48, 43), respectively, while the lowest one was observed in AP (10.98–15.38, 13.18), and KP (13.73–15.94, 14.83), respectively. Except for station NNP (18–21.17, 19.52), BC, similar to TC and TOC, revealed descending spatial distribution from the north to the south part of the region, with the highest and lowest value ( $\text{mg g}^{-1}$ ) in stations GP (22.52–25.68, 23.72) and AP (9–12.61, 10.81), respectively. By contrast what was observed for TC, TOC and BC, TN revealed heterogeneous distribution and varied between 2.43 and 4  $\text{mg g}^{-1}$  with an overall mean of 3.38  $\text{mg g}^{-1}$ . The mean C/N values varied between 3 and 14 with a total mean of 7.49. The higher value  $> 10$  was only observed in BAB (8.80–14, 11.51), and in other stations was  $< 10$ . These findings generally reflecting different inputs of OM, plausible post-depositional biodegradation and possibly hydrodynamic sorting processes (Meyers, 2003; He et al., 2018).

### 3.2. Spatial variability of aliphatic hydrocarbons

The total *n*-alkane concentrations ( $\Sigma_{22}\text{AHs}$ ,  $\mu\text{g g}^{-1}$  dw) varied from 405 to 220,626 (mean: 22169), and 664 to 145285 (16186) for coastal sediments and tar balls, respectively (Fig. 3, Table S4). One-way ANOVA revealed significant difference ( $p < 0.05$ ) in  $\Sigma_{22}\text{AHs}$  concentration in sediments and tar balls among sites. These immense ranges may be created by the complexity of this environment in terms of sedimentation, cycling and microbial degradation processes, organic matter and hydrocarbon sources (Kostka et al., 2011; Wang et al., 2015;

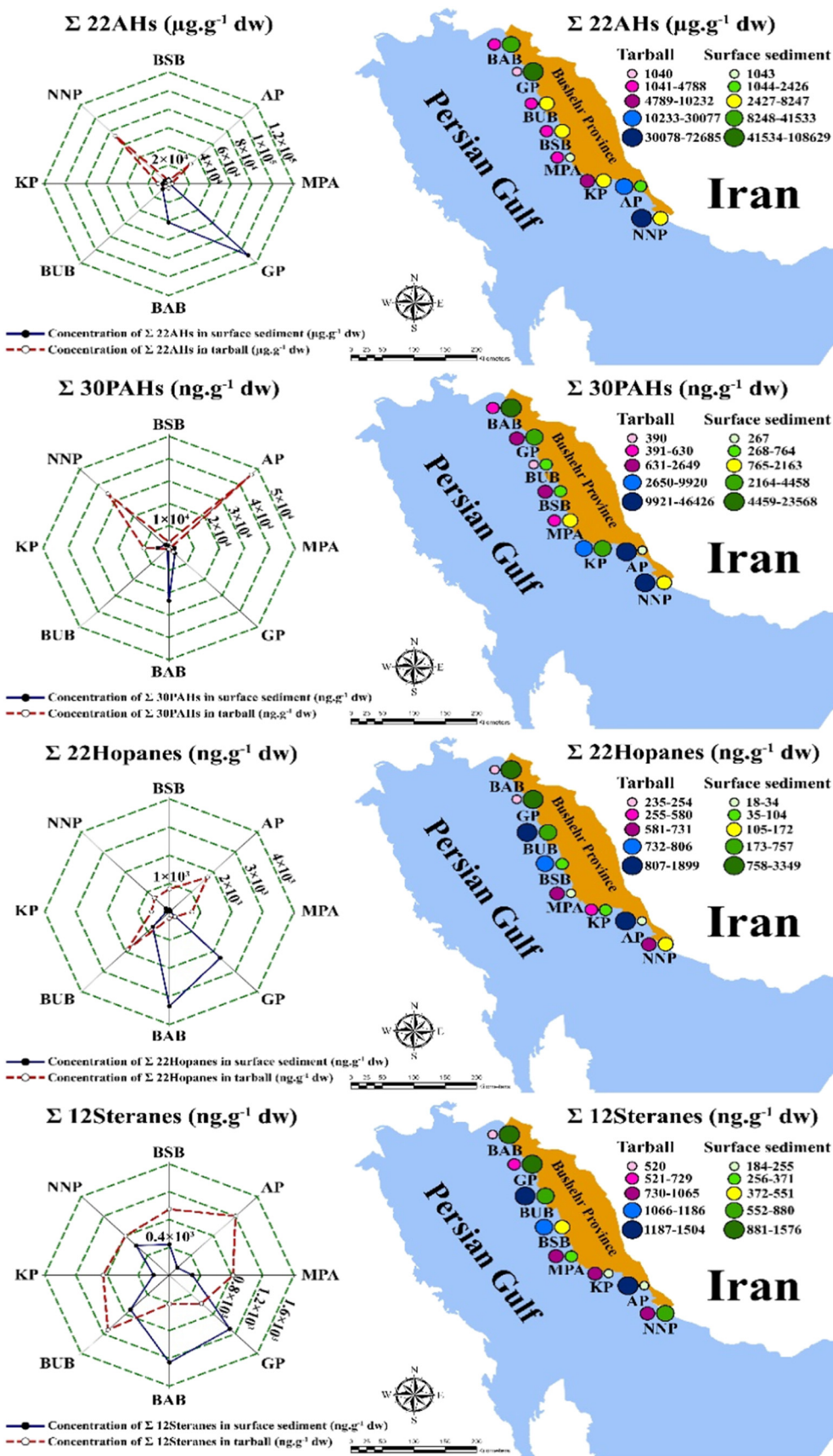


Fig. 3. Spatial distributions of petroleum biomarkers:  $\Sigma 22n$ -alkanes,  $\Sigma 30$ PAHs,  $\Sigma 22$ hopanes and  $\Sigma 12$ steranes of the coastal surface sediments and tar balls in the Bushehr Province, Persian Gulf.

He et al., 2018). The highest  $\Sigma_{22}$ AHs concentration ( $\mu\text{g g}^{-1}$  dw) in coastal sediments was found at station GP (33946-220626, 108629) located in the Genaveh harbor, pointing to a plausible source from intensive natural and human activities such as overflowing of various seasonal rivers to beaches with different sources of pollution, harboring of ships for transportation of oil and fishing, loading and refueling of vessels, discharging of ballast water of vessels, occasional oil spills from vessels, discharging of industrial and sanitary wastewater and transfer pipelines of oil and gaseous condensate, whereas, the maximum one in tar ball was measured in NNP (23328-145285, 72,685  $\mu\text{g g}^{-1}$  dw), due to industrial facilities, oil tanker transportation, and the concentration and trapping of contaminations in the area due to the indentations of the shore (Fig. 3, Table S4). In addition, the lowest  $\Sigma_{22}$ AHs concentration ( $\mu\text{g g}^{-1}$  dw) in coastal sediment and tar ball were observed at MPA.

\*note that greater circle shows higher amount of sand in samples in comparison to others.

(459-1444, 1043) and GP (664-1352, 1040), respectively. As can be seen in Fig. 3, with exception of NNP and MPA, a clear spatial increase pattern is observable for the concentrations of the *n*-alkanes in coastal sediments, which mounted from the south toward the west part of the BP. However, tar ball samples revealed no obvious trend. Compared to other sampling sites, concentrations in most samples of GP, BAB, and BUB were significantly higher ( $P < 0.05$ ) and these results were consistent with predominance of hydrocarbon inputs into these sites. It is well proved that total aliphatic hydrocarbons value of  $< 10 \mu\text{g g}^{-1}$  dw, 10–100  $\mu\text{g g}^{-1}$  dw and  $> 500$  represent respectively non-contaminated, moderated and significant contaminated sediments (Commendatore et al., 2012; Wang et al., 2011).

Having these criteria in mind, it can be deduced that the concentration levels of *n*-alkanes in all stations are significantly polluted. The overall average  $\Sigma_{22}$ AHs concentration ( $\mu\text{g g}^{-1}$  dw) in this study were higher than those found in the Persian Gulf, Iran, such as Kharg and Lark Islands (171–754, 57.99–232) (Ranjbar Jafarabadi et al., 2018a), Iranian coral Islands (385–937) (Ranjbar Jafarabadi et al., 2017a), Kharg Island (19.75–49.25) (Akhbarizadeh et al., 2016), Shadegan Wetland (395.3–14,933) (Bemanikharanagh et al., 2017), Northern Persian Gulf (ND to 1.71) (Mohebbi-Nozar et al., 2015). On the other hand, the average total *n*-alkane concentrations were relatively comparable to heavily polluted sites, such as Barataria Bay, Gulf of Mexico (77,399  $\mu\text{g g}^{-1}$ ) (Kirman et al., 2016); sediments in Vietnam (1056–34,794  $\mu\text{g g}^{-1}$ ) (Duong et al., 2014); Gulf of Mexico (0.050–535,000  $\mu\text{g g}^{-1}$ ) (Sammarco et al., 2013).

Saturated hydrocarbons, *n*-alkanes, in the environment have intricate origins. Some general criteria to determine the possible origins (anthropogenic or natural) of organic compounds have been used (Ranjbar Jafarabadi et al., 2017a; de Souza Neto et al., 2008; Mille et al., 2007). GC traces demonstrated regular distribution varied from *n*-C<sub>14</sub> to *n*-C<sub>33</sub> alkanes with equivalent distribution pattern of both odd-carbon numbered alkanes and even-carbon-numbered alkanes (Fig. S1). As a matter of fact, GC trace analysis exhibited a unimodal and bimodal *n*-alkane distribution at most sampling sites. Both unimodal and bimodal *n*-alkane distributions ranging from *n*-C<sub>11</sub> to *n*-C<sub>35</sub> are characteristics of petroleum origin (Ranjbar Jafarabadi et al., 2017a). It may also be due to the superposition of two different types of petroleum product sources (Yang et al., 2009), and this is more probable for some sediments of BAB, and GP, considering the nature of the petroleum products input and the intense maritime activities in this region. Total *n*-alkane concentration in this coastal system was high especially in sites with higher anthropogenic activities, which could be ascribable to the massive proportions of lower chain *n*-alkanes than their higher homologues. The concentration of *n*-C<sub>21</sub> to *n*-C<sub>33</sub> hydrocarbons in all stations was more concentrated than the shorter chain *n*-alkanes (*n*-C<sub>14</sub> to *n*-C<sub>20</sub>). For sediments, the relatively high concentrations of long chain *n*-alkanes, with a peak in *n*-C<sub>29</sub> (followed by *n*-C<sub>30</sub>, *n*-C<sub>33</sub>) were detected at the stations. In tar ball, except for NNP with a pick in *n*-C<sub>21</sub>

and *n*-C<sub>23</sub>, high concentrations of long chain *n*-alkanes with a peak in *n*-C<sub>31</sub> and *n*-C<sub>32</sub> were identified at all sites. In the current study, *n*-C<sub>6</sub> to *n*-C<sub>10</sub> were not detected and this absence may be due to their evaporation, which is totally observed in lower molecular weight (LMW) hydrocarbons.

To decipher spatial variations of *n*-alkane sources more precisely, multiple deterministic ratios were computed (Table S4). The value of low molecular weight to high molecular weight ratio (LMW/HMW)  $< 1$  usually indicates *n*-alkanes produced by higher plants, marine animals, and sedimentary bacteria (Wang et al., 2006), while LMW/HMW ratios close to 1 and  $> 2$  suggest *n*-alkanes that are mostly from petroleum and plankton sources and also the presence of fresh oil input, respectively (Commendatore et al., 2000). Nonetheless, since LMW hydrocarbons would degrade preferentially, the presence of heavier oil or more degraded crude oil could result in lower ratios of LMW/HMW  $< 1$  (Commendatore et al., 2000). The LMW/HMW ratios in sediments varied between 0.24 (GP) and 0.92 (MPA) and totally were all  $< 1$ , whereas in tar balls except for station NNP (1.24), all stations were  $< 1$  (0.23 (GP) - 0.65 (BAB)), reflecting the more origin of higher plants, marine animals, and sedimentary bacteria.

Another indicators of OM sources are the carbon preference indices (CPI), PETRO, PLK and TER (Ranjbar Jafarabadi et al., 2017a; He et al., 2018). Carbon Preference Index (CPI), which is defined by odd to even *n*-alkanes (C<sub>11</sub>-C<sub>35</sub>), has been widely used as a robust indicator to demonstrate petroleum contamination in sediments (Ranjbar Jafarabadi et al., 2017a, 2018a; He et al., 2018; Akhbarizadeh et al., 2016; Resmi et al., 2016). Regarding this, petrogenic hydrocarbons indicate CPI values close to 1, whilst *n*-alkanes derived from terrestrial vascular plants generally have CPI values varying between 3 and 6 (Pearson and Eglinton, 2000; Wang and Fingas, 2003; Liu et al., 2012). CPI values varied from 0.67 (KP) to 1 (AP) in sediment and 0.74 (MPA) to 1.23 (BSB) over the course of the study, confirming that there were intensive effects from petroleum sources at most stations (Ranjbar Jafarabadi et al., 2017a, 2018a; Resmi et al., 2016) (Table S2) and several studies have confirmed oil CPI values to be around 1.0 (Bemanikharanagh et al., 2017; Ranjbar Jafarabadi et al., 2017a, 2018a; Resmi et al., 2016; Kalaitzoglou et al., 2004). The CPI<sub>25–35</sub>, the odd to even HMW-*n*-alkanes (C<sub>25</sub>-C<sub>35</sub>), has been continuously applied to recognize vascular plant wax contribution versus fossil fuel contamination (Aboul-Kassim and Simoneit, 1996; Ranjbar Jafarabadi et al., 2017a; He et al., 2018). The CPI<sub>25–35</sub> showed no specific spatial variation and oscillated from 2.13 to 2.23 and 2 to 2.50 in sediment and tar ball samples respectively, confirming to some extent vascular plant wax contribution. In contrast to CPI<sub>25–35</sub>, CPI<sub>11–20</sub> (the odd to even LMW-*n*-alkanes (C<sub>11</sub>-C<sub>20</sub>)) values in most sediment and tar ball samples were  $< 1$  or close to 1.0, suggesting inputs from fossil fuel hydrocarbons as well as bacterial activities (Pearson and Eglinton, 2000; Ranjbar Jafarabadi et al., 2017a; He et al., 2018).

The sum of petroleum-derived (even *n*-alkanes from C<sub>12</sub> to C<sub>20</sub>, PETRO), phytoplankton- (odd *n*-alkanes from C<sub>15</sub> to C<sub>21</sub>, PLK), and terrestrial- (odd *n*-alkanes from C<sub>23</sub> to C<sub>33</sub>, TER) *n*-alkanes were computed to evaluate the proportion/dominance of them (Ranjbar Jafarabadi et al., 2017a, 2018a; He et al., 2018) (Fig. 4, Table S4). In all coastal sediments, the terrestrial (TER) and petroleum (PETRO)-derived *n*-alkanes were the dominant, with the highest value at GP (TER: 36948  $\mu\text{g g}^{-1}$  dw, 67%; PETRO: 12536, 23%), whereas tar ball samples had more phytoplankton sourced *n*-alkanes with the higher level at BUB (PLK: 6005, 58%) (Fig. 4, Table S4).

Another effective indicator of petroleum contamination is a mixture of structurally complex isomers of homologous branched and cyclic hydrocarbons that cannot be resolved by capillary columns and called unresolved complex mixture (UCM) (Brassell et al., 1980; Ranjbar Jafarabadi et al., 2017a, 2018a; He et al., 2018). This indicator originates from degraded petroleum (Brassell et al., 1980), chronic emission of vehicles, and volatiles from diesel (Simoneit, 1989; Gough and Rowland, 1990; Tolosa et al., 2005; Mille et al., 2007), and bacteria-

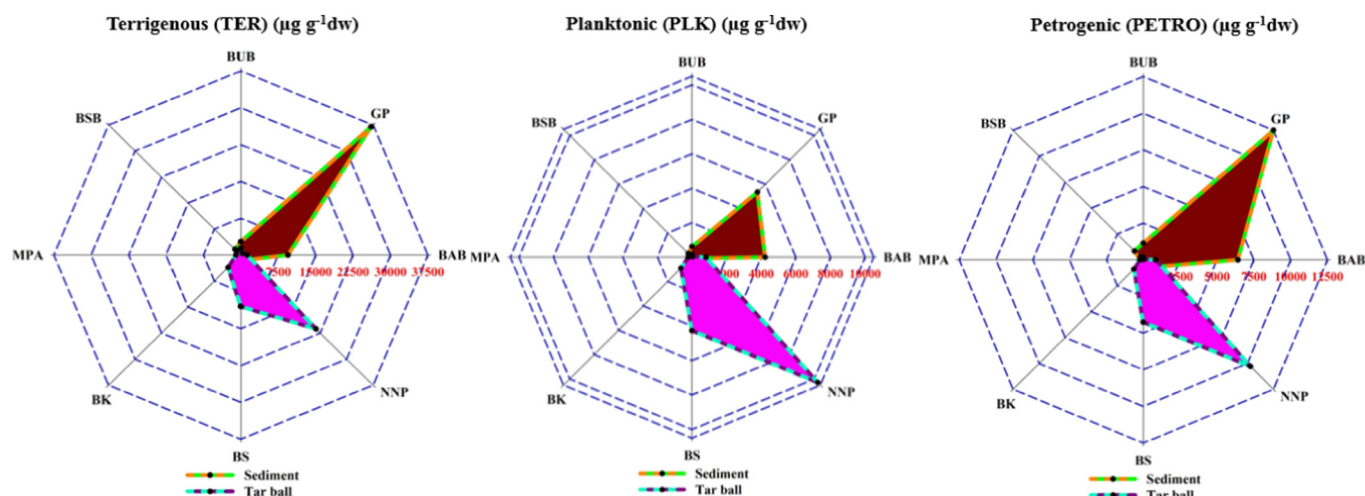


Fig. 4. Indices calculated from *n*-alkane biomarkers including Terrigenous (TER), Planktonic (PLK) and Petrogenic (PETRO) in the coastal surface sediments and tar balls of the Bushehr Province, Persian Gulf.

derived UCMs (Bouloubassi et al., 2001). In the present study, the UCM was evident in most sediment (more) and tar ball samples and varied from 519,242 (AP) to 24712028 (GP)  $\mu\text{g g}^{-1}$  dw and 328758 (GP) to 15609747 ((NNP)  $\mu\text{g g}^{-1}$  dw in sediment and tar ball samples, respectively. The highest concentrations were found in stations GP and NNP for sediment and tar ball samples, consistent with total significant petroleum inputs at these locations as pointed out earlier. In addition to UCM, U/R, a useful tool to identify the presence of degraded petroleum hydrocarbons (Ranjbar Jafarabadi et al., 2017a, 2018a), was calculated and were  $> 2$  at all sites, varied between 262 and 808  $\mu\text{g g}^{-1}$  dw (sediment) and 180 to 654 (tar ball), demonstrating a significant contamination by petroleum products (Simoneit and Mazurek, 1982; Gogou et al., 2000; Ou et al., 2004). Overall, although heavy weathering eliminates LMW-*n*-alkanes and modifies UCM toward HMW, UCM in the lower chain-length end ( $< C_{20}$ ) is associated with slightly weathered petroleum (Jacquot et al., 1999; Lima et al., 2012). UCM occurred as both short-chain ( $C < 20$ ) and long chain ( $C > 25$ ) hydrocarbons in most sediment samples, but occurred predominantly as long-chain hydrocarbons in all the most tar ball samples (Fig. S1), reflecting a combination of slightly and extremely weathered petroleum in coastal sediments and extremely weathered petroleum contamination in tar balls. In the light of microbial reworking is an additional source of UCM on the short-chain end (Carstensen et al., 2015), it could be another sources of UCM in sediments, nonetheless, due to UCM derived from microbial reworking is a process longer than a year, the UCM ignored in this study should be driven by petrogenic input (He et al., 2018). This distribution of UCM in sediments is also reported in another studies all around the world (Li et al., 2015; Maciel et al., 2016; Zhao et al., 2014; Ranjbar Jafarabadi et al., 2017a; He et al., 2018).

The terrigenous/aquatic ratio (TAR) has been broadly applied to appraise the relative significance of terrestrial against aquatic inputs (Mille et al., 2007). The TAR values were  $> 1$  for all sediment and tar ball samples, corroborating the preferential preservation of terrestrial hydrocarbons over planktonic ones in the coastal area of the region. Similar to Ranjbar Jafarabadi et al. (2017a),  $\Sigma_{22}\text{AHs}/n\text{-C}_{16}$  and odd even carbon number predominance (OEP) were also calculated and ranged from 17.25 to 296 and 5550 to 78334220 in sediment samples, respectively, whereas in tar balls varied respectively from 29.87 to 88.76 and 3537 to 21227864, pointing to intensive terrestrial hydrocarbon inputs.

### 3.2.1. Spatial variability of petroleum biomarkers

The mean concentration ( $\text{ng g}^{-1}$  dw) of  $\Sigma_{22}$ hopanes and  $\Sigma_{12}$ steranes oscillated from 18.17 (AP) to 3349 (BAB) (overall mean: 853) and

184.66 (AP) to 1578 (BAB) (743) in costal sediments, whereas ranged from 235 (BAB) to 1899 (BUB) (864) and 520 (BAB) to 1504 (AP) (1052) in tar balls, suggesting higher accumulation of petroleum biomarkers in tar balls relative to sediments. Moreover, for sediments, station BAB displayed higher values, while for tar balls stations AP and BAB indicated more levels of these pollutants. Additionally, the mean concentration ( $\text{ng g}^{-1}$  dw) of  $\Sigma_{30}\text{PAHs}$  was totally significantly lower than  $\Sigma\text{AHs}$ , and higher than  $\Sigma\text{hopanes}$  and  $\Sigma\text{steranes}$  and varied from 267 (AP) to 23,568 (BAB) with a total mean of 4650  $\text{ng g}^{-1}$  dw for coastal sediment samples, whereas varied between 390 (BAB) and 46,426 (AP) (overall mean: 12167) for tar balls in the whole study area (Fig. 2, Table S4). Similar to  $\Sigma\text{AHs}$ , one-way ANOVA revealed spatial significant differences ( $p < 0.05$ ) in  $\Sigma_{30}\text{PAHs}$  concentration among stations. In addition, one sample *t*-student test showed considerably significant variation ( $p < 0.05$ ) in accumulation of PAHs in sediment and tar ball samples at each station, separately. These ranges ( $\text{ng g}^{-1}$  dw) were larger than other studies in the Persian Gulf, Iran, such as Lark (16.56–487) and Kharg (41.61–693) Islands (Ranjbar Jafarabadi et al., 2018a; Khaksar et al., 2019), Kharg Island (2.95–253.3) (Akhbarizadeh et al., 2016), Bushehr Peninsula (285.9–1288) (Aghadadashi and Mehdinia, 2016), Asaluyeh Port (1.8–81.2) (Keshavarzifard et al., 2017), Imam Khomeini Port (2631–5148) (Abdollahi et al., 2013), Bushehr Port (356–611) (Mehdinia et al., 2015), Persian Gulf (10.33–186.16) (Khazaali et al., 2015), Bushehr Creeks (371–611) (Mehdinia et al., 2015) and also in Chabahar Bay, Oman Sea, Iran (nd-92.8) (Agah et al., 2017), and were lower than in sediments in Shadegan wetland (593.74–53,393) (Bemanikharanagh et al., 2017), confirming totally higher anthropogenic inputs in coastal area of BP. By comparing the pollution levels defined by Baumard et al. (1998), stations AP, BSB and BUB were characterized by moderate (100–1000  $\text{ng g}^{-1}$  dw) pollution, while other stations were considered high (1000–5000  $\text{ng g}^{-1}$  dw) (GP, MPA, KP, NNP) to extremely high ( $> 5000$   $\text{ng g}^{-1}$  dw) (BAB) pollution.

One-way ANOVA showed spatial significant difference ( $p < 0.05$ ) in concentration of  $\Sigma_{16}\text{PAHs}$ ,  $\Sigma\text{PPAHs}$  and  $\Sigma\text{APAHs}$  in sediment and tar ball samples among stations. One sample *t*-test revealed parent PAHs were more abundant than the Alkyl homologues of the total PAHs in all sediment samples, while in tar balls, except for stations KP, AP and NNP, the Alkyl homologues were higher than the parent PAHs of the total PAHs in all sites ( $p < 0.05$ ). Mean concentration ( $\text{ng g}^{-1}$  dw) of  $\Sigma_{16}\text{PAHs}$  varied from 107 (AP) to 106,091 (BAB) with a total average of 14,359 in surface sediment, whereas in tar balls oscillated from 134 (BUB) to 13,512 (AP) (2871).  $\Sigma\text{PPAHs}$  were 515 (88.73% of the  $\Sigma_{30}\text{PAHs}$ ) (BSB) to 24,258 (70.58%) (BAB) and 44 (79%) (BAB) to

25,812 (44%) (AP) in sediment and tar ball samples, respectively. ΣPAHs varied between 48 (3.95%) (MPA) and 4982 (29.41%) (BAB) in sediment, whereas varied between 326 (46%) (BUB) and 19,204 (56%) (AP) in tar ball (Table S4). The plausible cause was that the PAHs in the north western part of the study area which was originated from largely industrial infrastructures especially petroleum fields are mainly less in these areas (south western), and it might be probably said that the residence time of PAHs in sampling sites with lower concentrations is less than those with higher concentrations. Hereupon, it could be claimed that less depositional PAHs were accumulated in the sediments.

The composition profile of PAHs by ring number is illustrated in Fig. 6. Although the proportion of 2- and 6- ringed hydrocarbons showed a wide variation with no specific trend (Table S4), one-way ANOVA revealed significant difference ( $P < 0.05$ ) in LMW/MMW/HMW-PAHs accumulation in both sediments and tar balls. The coastal sediment PAH profiles were significantly dominated by HMW-PAHs in stations BAB (78% of the total PAHs), GP (66%) and BUB (61%), while stations KP (40%), NNP (57%), and BAB (82%) exhibited higher proportion of LMW-PAHs. MMW-PAHs were only dominated in MPA (58%). In tar ball samples, except for NNP (57%), other stations demonstrated the dominance of HMW-PAHs (40–69%) (Fig. 5, Table S4). The observed pattern may be explained in terms of adjacency to the source and physicochemical properties of PAHs (Ranjbar Jafarabadi et al., 2017a; Rahmanpoor et al., 2013). On the one hand, noticeable predominance of LMW-HMW PAHs is comprehensible for some stations such as BAB, GP, BUB, and KP since they are subject to majorly petrochemical and petroleum transport by huge vessels which is considered as a core of industrial activities. To recognize potential sources of PAHs, several common diagnostic ratios were calculated (Fig. 6, Table S4). The diagnostic ratios of Ant/(Ant + Phe), BaA/(BaA + Chr), Flu/(Flu + Pyr), MPhe/Phe, Phe/Ant, and LMW/HMW in coastal sediments and tar balls are plotted in Fig. 6. MPhe/Phe ratio is the most leading criteria to separate the petrogenic (2–6) from pyrogenic ( $< 1$ ) origin (Ranjbar Jafarabadi et al., 2017a, 2018a; Prah and Carpenter, 1983; Zakaria et al., 2002). In this study, MPhe/Phe ratio demonstrated a wide range in sediment (47.92–108.97, mean: 83.69) and tar ball (21.25–248, 96), reflecting probably petrogenic source. Phe/Ant  $< 10$  is considered as a pyrogenic source, while  $> 10$  indicates petrogenic one (Parlanti, 1990; Soclo et al., 2000) and this ratio were 2.37 to 10.71 (5.26) in sediment and 2.22 to 13.79 (7) in tar ball, reflecting the petrogenic source only in station GP for sediment and NNP for tar ball.

LMW/HMW was  $< 1$  at most sediment samples except for AP (6.13) and NNP (1.24), while in tar balls except for BAB (0.09), GP (0.27) and BSB (0.86) were  $> 1$  in another stations, confirming pyrogenic origin for most coastal sediments and petrogenic one for tar balls (Baumard et al., 1998; Budzinski et al., 1997; Sicre et al., 1987; Soclo, 1986; Yunker et al., 2002b). In this study, also isomeric ratios were calculated to differentiate PAHs in samples from petroleum and combustion sources (Fig. 6).

Ant/Ant + Phe ratio less and higher than 0.1 illustrate pyrogenic and petrogenic sources, respectively (Yunker et al., 2002a) and were mostly  $> 0.1$  at both sediment and tar ball samples, suggesting pyrogenic source. BaA/(BaA + Chr) ratio was between 0.2 and 0.35 at most sediment and tar ball samples in all stations, reflecting petroleum combustion, including liquid fossil fuels, vehicle, and crude oil combustion (Ranjbar Jafarabadi et al., 2017a). Flu/(Flu + Pyr) were 0.17 to 0.42 in sediments and 0.08 to 0.37 in tar balls, reflecting petroleum source (Dvorská et al., 2011; Yunker et al., 2002b; Zhang et al., 2004). InP/(InP + BghiP) varied respectively from 0.14 to 0.44 and 0.16 to 0.49 in sediment and tar ball, suggesting petroleum combustion (Yunker et al., 2002a).

However, it is noteworthy that these diagnostic ratios sometimes come with multiple explanations, especially in aquatic environments (Yunker et al., 2002b; Martinez-Silva et al., 2018). Examples of inconsistencies based on PAH diagnostic ratios have been reported in Persian Gulf, Iran (e.g., Ranjbar Jafarabadi et al., 2017a). Therefore, our study area serves as another system that these PAH diagnostic ratios may not work perfectly in tracking sources of PAHs. It further suggested that sources of PAHs may differ to those of aliphatic hydrocarbons, and implied that data interpretation in coastal systems like this could be strongly biased if only one group of biomarkers was used.

### 3.2.2. Spatial variability of petrogenic biomarkers: Hopanes, steranes, gammacerane, $\beta$ -carotane, pristane and phytane

In this study, in addition to the *n*-alkanes derived indices, the presence of petrogenic hydrocarbons is further calculated through the identification of a suit of petroleum and fossil carbon related biomarkers, comprising pristane (Pri), phytane (Phy), the hopane and sterane series, gammacerane and  $\beta$ -carotane (Fu and Guoying, 1989; Volkman et al., 1992). Pri can generate from zooplanktons and/or marine animals, while phytane originates from petroleum hydrocarbons (Gomez-Belinchon et al., 1988; Gao et al., 2007). Moreover,

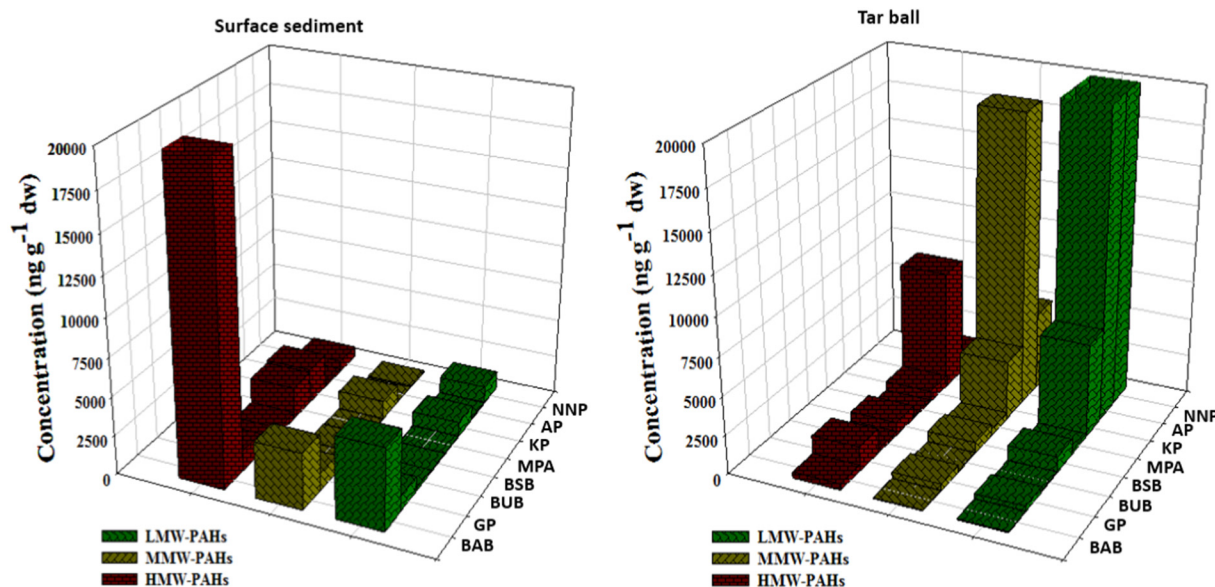


Fig. 5. Concentration of LMW, MMW and HMW-PAHs (based on  $\text{ng g}^{-1} \text{dw}$ ) in the coastal surface sediment and tar balls in sampling sites from Bushehr Province, Persian Gulf.

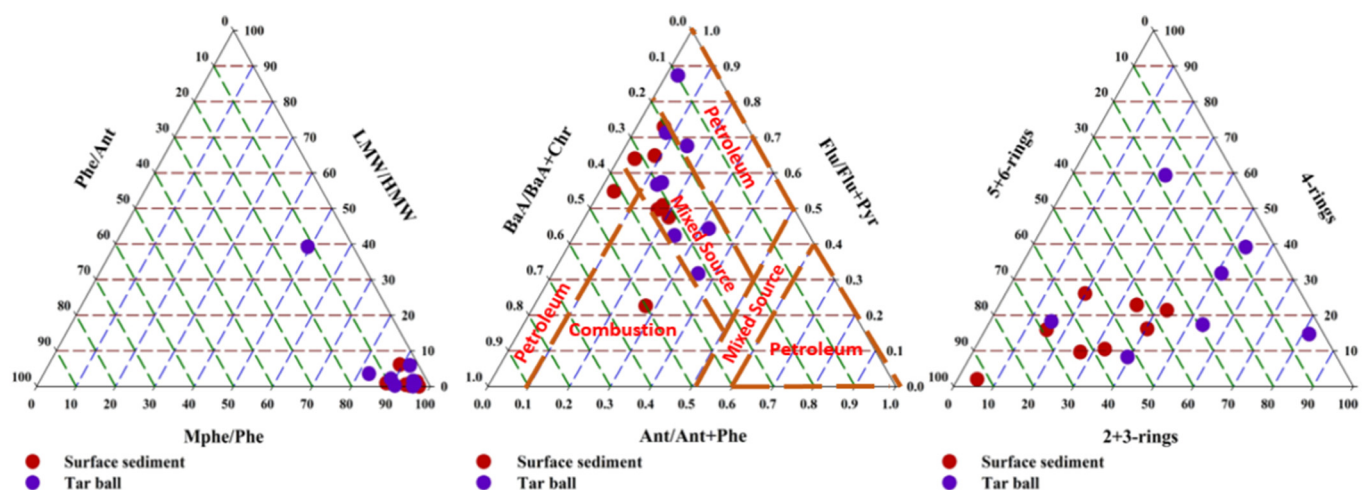


Fig. 6. Diagnostic ratios based on PAH parents and isomers for source identification in coastal surface sediment and tar balls in Bushehr Province, Persian Gulf.

reduction or oxidation of chlorophyll may generate pristane and phytane (Mille et al., 2007). Pri/Phy ratio was 0.25 to 1.51 with a total mean of 0.65 and 0.36 to 1 (0.63) in coastal sediment and tar ball samples, respectively, suggestive of petrogenic OM inputs (Ranjbar Jafarabadi et al., 2017a, 2018b; He et al., 2018). In addition, Pri/ $n$ -C<sub>17</sub> and Phy/ $n$ -C<sub>18</sub> varied respectively from 0.51 to 1.73 (1.10) and 0.45 to 1.81 (0.91) in sediments and 0.57 to 2.83 (1.22) and 0.34 to 1.76 (1) in tar balls. Much lower ratios of Pr/ $n$ -C<sub>17</sub> and Ph/ $n$ -C<sub>18</sub> in the coastal sediment ( $< 1$ ) than in the tar balls ( $\geq 1$ ) were extremely related to the presence of less degraded or relatively fresh oil hydrocarbons particularly in BUB, KP, and NNP, while for tar balls imply the presence of degraded petroleum hydrocarbons (Gao et al., 2007; Pavlova and Papazova, 2003; Mille et al., 2007; Commendatore et al., 2012). Over and above that, hopanes and steranes were identified in all sediment and tar ball samples. The robust correlation ( $R^2 = 0.86$ – $0.91$ ,  $P < 0.002$ ) between hopanes and steranes suggested their analogous sources and common dynamic processes from the sediment and tar ball samples in the coastal area studied.

The C<sub>30</sub> homologues (17a(H), 21b(H)-hopane (C<sub>30ab</sub>); 17b(H), 21a(H)-hopane (C<sub>30ba</sub>)) followed by C<sub>29</sub> homologues (17a(H), 21b(H)-30-norhopane (C<sub>29ab</sub>); 17b(H), 21a(H)-30-norhopane (C<sub>29ba</sub>)) and Gammacerane, a nonhopanoid C<sub>30</sub> triterpane, were detected in all sediment and tar ball samples and were the most abundant hopanes in most samples, in particular those collected from intensive industrial activities. This compounds are totally found in most crude oils formed in marine sediments and is reported in the Persian Gulf (Ranjbar Jafarabadi et al., 2017a). Besides, *B*-Carotane that derived from carotenoids in microbes or photosynthetic plants, was identified in most of samples particularly tar balls, with the highest concentration at BUB followed by AP. This compound has found in several coastal oil sands (Wang et al., 2013) and is broadly applied as an indicator of petroleum inputs (Fu and Guoying, 1989; Chen et al., 1996).

Ts (18a(H)-22, 29, 30-trisnorhopane) to Tm (17a(H)-22, 29, 30-trisnorhopane), the hopane index, is a useful criterion which has been used to determine the source and the plausible degree of maturation of crude oil (Hu et al., 2009; Louati et al., 2001; Shirneshan et al., 2016). In addition, the 22S/(22S + 22R) ratio has been also confirmed to be an efficacious evidence of fossil fuel input (Hu et al., 2009). Tm/Ts ratio, varied mostly from 0.20 to 1.10 (0.75) and 0.52 to 0.81 (0.77) in sediment and tar ball samples, respectively (Table S4). The ratios of 22S/(22S + 22R) epimers of  $\alpha\beta$ C<sub>31</sub> homohopanes showed a narrow range of 0.41–0.47 in sediment and a wide range of 0.24–0.97 in tar balls, confirming full maturity of oil (Mackenzie, 1984), consisting with other studies all over the world (Ranjbar Jafarabadi et al., 2017a; He et al., 2018; Hu et al., 2009; Pang et al., 2003). These conclusions indicate

these biomarkers and proxies, the petrogenic hydrocarbon inputs in this region were either from oil pollution most likely contributed by occasional oil spills due to intense traffic of ships, or fossil organic carbon from coastal areas of Bushehr Province with similar biomarker distributions.

### 3.3. Further statistical analysis

#### 3.3.1. PCA

In the present study, the PCA analysis was specifically on *n*-alkanes, PAHs and biomarkers (hopane and sterane) to further investigate their sources in coastal sediments and tar balls (Fig. S2). The results from PCA for *n*-alkanes exhibited three components; two PCs explained 81.5% of the total variance, whereas the third PC accounted for 18.5%. The PC<sub>1</sub>, accounted for 44.25% of total variance, demonstrated a considerably high positive loading of the variables of long-chain *n*-alkanes HMW-AHs. LMW-AHs contained more even-numbered-carbons such as *n*-C<sub>18</sub>, *n*-C<sub>20</sub> and some odd-numbered ones including *n*-C<sub>17</sub>, *n*-C<sub>19</sub>, ascribable to high terrestrial and relatively petrogenic sources (Ranjbar Jafarabadi et al., 2017a, 2018a). The PC<sub>2</sub> responsible for 35.1% of total variance and was distinguished by the high positive loadings of HMW-*n*-alkanes (*n*-C<sub>22</sub> to *n*-C<sub>33</sub>). This could be elucidated by their source, mixed and probably of marine biogenic contributions (Ranjbar Jafarabadi et al., 2017a). Besides, the moderate-chain alkanes (*n*-C<sub>22</sub> to *n*-C<sub>26</sub>) are mainly derivatives from marine aquatic and bacterial activities, such as bacterial degradation (Ranjbar Jafarabadi et al., 2017a). PC<sub>3</sub> associated with *n*-C<sub>15</sub> and *n*-C<sub>17</sub> that might be ascribable to some depleted marine bacteria (Grimalt and Albaigés, 1987; Ranjbar Jafarabadi et al., 2018a).

Similar to *n*-alkane, PCA also performed for PAHs and revealed three factors. The PC<sub>1</sub>, PC<sub>2</sub> and PC<sub>3</sub> elucidated by 51.0%, 35.5% and 13.5% of the total variance. Component matrix identified by PCA demonstrated that the first and second components (PC<sub>1</sub>, PC<sub>2</sub>) have high correlations with HMW (e.g., 5 and 6-rings PAHs) and LMW-PAHs, respectively, whilst MMW-PAHs (4-rings) was well correlated with the third component (PC<sub>3</sub>) (Fig. S2). Therefore, the study areas had numerous sources of PAHs, chiefly from fossil combustion and natural oil seeps. All together all the result obtained from analysis confirmed the high petrogenic footprint in all study area.

The separation between the hopane and sterane compound patterns of coastal sediments, and tar balls in PCA analyses (Fig. S2) revealed that the sources of hopane and sterane were most likely petrogenic. The results showed that the PC<sub>1</sub> responsible for 59% and 63% of total variances, predominately weighted by HC<sub>29</sub>, HC<sub>30</sub> (hopane) and 27 $\beta$ BS, 28 $\beta$ BR, 28 $\beta$ BS, 28 $\alpha\alpha$ R (sterane) for sediment and tar ball samples.

Hereupon, the PC<sub>1</sub> represents the sources of petroleum spill. Several oilfields, petrochemical factories and refineries located near most stations, may contribute substantially to oil pollutants by oil extraction and exploitation. PC<sub>2</sub> (30% and 27% of total variance for hopanes, and steranes) was distinguished by high loadings of SS and SR (C<sub>31</sub>, C<sub>32</sub>, C<sub>33</sub>, C<sub>34</sub>, Ts, and Tm) for hopane and 28ααR, 29ααS, 29ββR, 29ββS, 29ααR for steranes in coastal sediments and tar balls, typical markers of petroleum profile. Hereupon, PC2 can be identified as combustion of bio-fuels and fossil fuels. PC3 explained by 10% for hopane (correlated with HC<sub>1</sub>, HC<sub>2</sub>, HC<sub>3</sub>, HC<sub>4</sub>, HC<sub>5</sub>, HC<sub>6</sub>, HC<sub>7</sub>, HC<sub>8</sub>, SC<sub>35</sub>, RC<sub>35</sub>) and 11% for steranes (associated with 27ααS, 27ββR, 27ββS, 27ααR). Accordingly, PC<sub>3</sub> is apparently relative to crude oil processing facilities, transfer pipelines of oil and gaseous condensate, and petrochemical factories and oil and gas refinery.

There are totally 357 offshore wells in the Persian Gulf (Amir-Heidari and Raie, 2018) and most of these wells are located in the central and west part of the Gulf, which natural spills or anthropogenic activities such as crude oil extraction could impact on this area. Due to some limitation of data, in this study the authors could obtain information about only 4 oil wells. The cross-plot diagram of the diagnostic ratios of C<sub>29</sub>/C<sub>30</sub> versus ΣC<sub>31</sub>-C<sub>35</sub>/C<sub>30</sub> for hopanes and C<sub>28</sub> αββ/(C<sub>27</sub> αββ + C<sub>29</sub> αββ) versus C<sub>29</sub> αββ/(C<sub>27</sub> αββ + C<sub>28</sub> αββ) for steranes between all the tar balls and coastal sediments and also oil samples of Bahregansar, Soroush, Abuzar and Nowruz were used to identify the source of tar ball and coastal sediment samples (Fig. 7a, b) (Zakaria

et al., 2001; Yim et al., 2011; Suneel et al., 2014; Shirneshan et al., 2016). The results of both of the double ratio plots indicated that, Abuzar and to some extent Soroush and Bahregansar crude oil fall among the tar ball and sediment samples. In addition, to exhibit whether the source of contamination in tar ball and coastal surface sediment is from oil wells or rivers in the vicinity of the study area, and also to better separate the characteristics of the reference oils of Bahregansar, Soroush, Abuzar and Nowruz from the tar ball and coastal sediment samples, a PCA was performed using 22 parameters viz. *n*-alkane biomarkers (CPI, Pri/Phy, Pri/*n*-C<sub>17</sub>, Phy/*n*-C<sub>18</sub>, U/R), PAH biomarkers (MPhe/Phe, LMW/HMW, Chr/BaA, Fluo/Pyro, Phe/Ant, Ant/Ant + Phe, Fluo/Fluo + Pyr, BaA/BaA + Chr, Inp/Inp + Bghi), hopane and steranes biomarkers (C<sub>23</sub>/C<sub>30</sub>, Ol/C<sub>30</sub> (18α(H)-oleanane/C<sub>30</sub> 17α,21β-hopane), Ts/(Ts + Tm), C<sub>29</sub>/C<sub>30</sub>, C<sub>31</sub>S/(C<sub>31</sub>S + R), ΣC<sub>31</sub>-C<sub>35</sub>/C<sub>30</sub>, C<sub>28</sub>αββ/(C<sub>27</sub> αββ + C<sub>29</sub> αββ) and C<sub>29</sub> αββ/(C<sub>27</sub> αββ + C<sub>28</sub>αββ). The results demonstrated that two factors that were selected as the principal factors elucidated about 98.50% of the total variability in the diagenic ratios of the tar ball and coastal sediments and also crude oil samples (Fig. 7c). As can be seen in Fig. 7c, it is obvious that the Nowruz crude oil are far away from the remaining samples. This perspicuously reveals that the Nowruz crude oil cannot be the source candidates. It appears that, the tar ball and coastal sediment samples with Abuzar crude oil followed by soroush and Bahregansar oils fell close together. This strongly infers that the tar ball and coastal sediment samples were originated from the Abuzar (more), Soroush and Bahregansar oils.

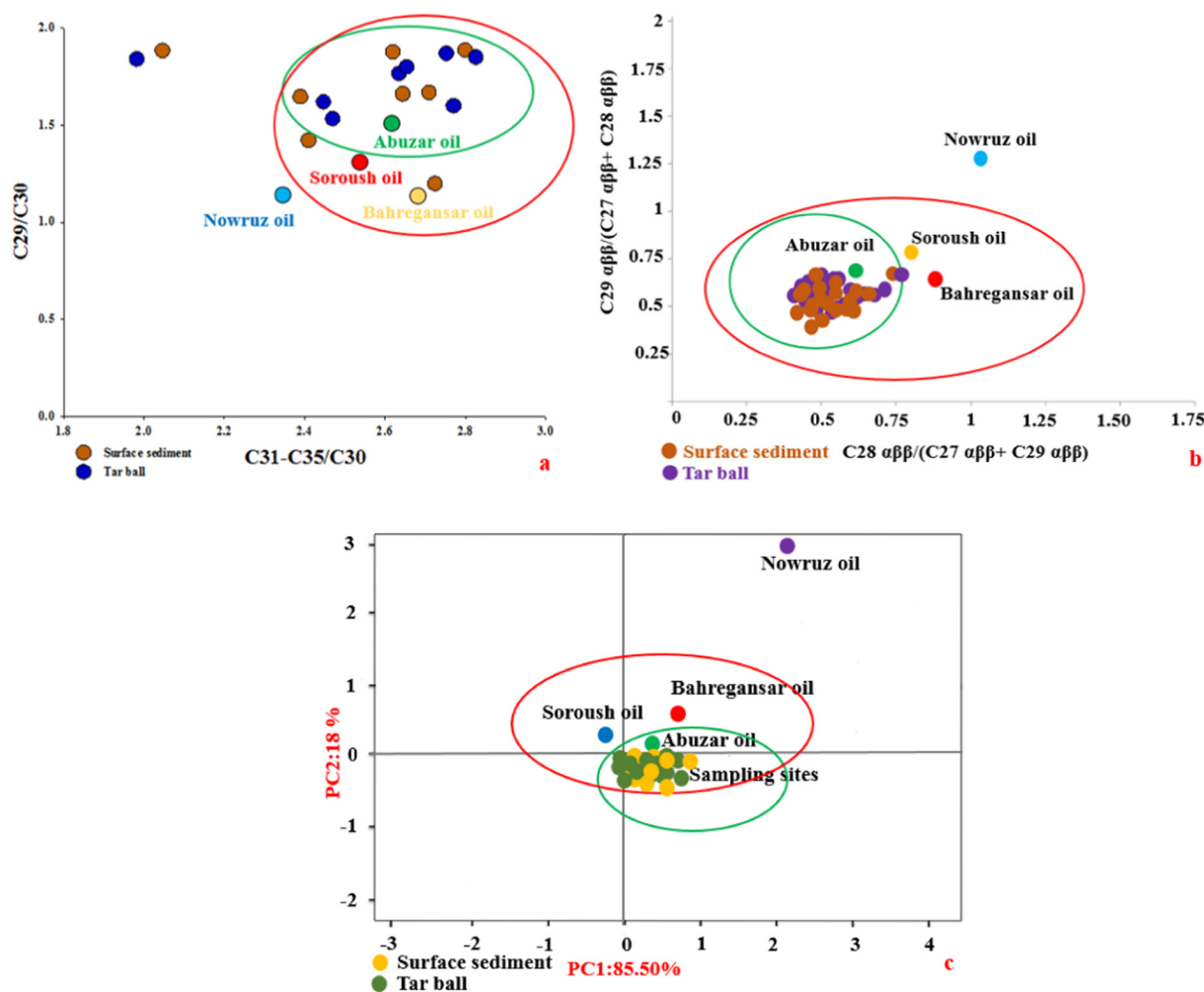
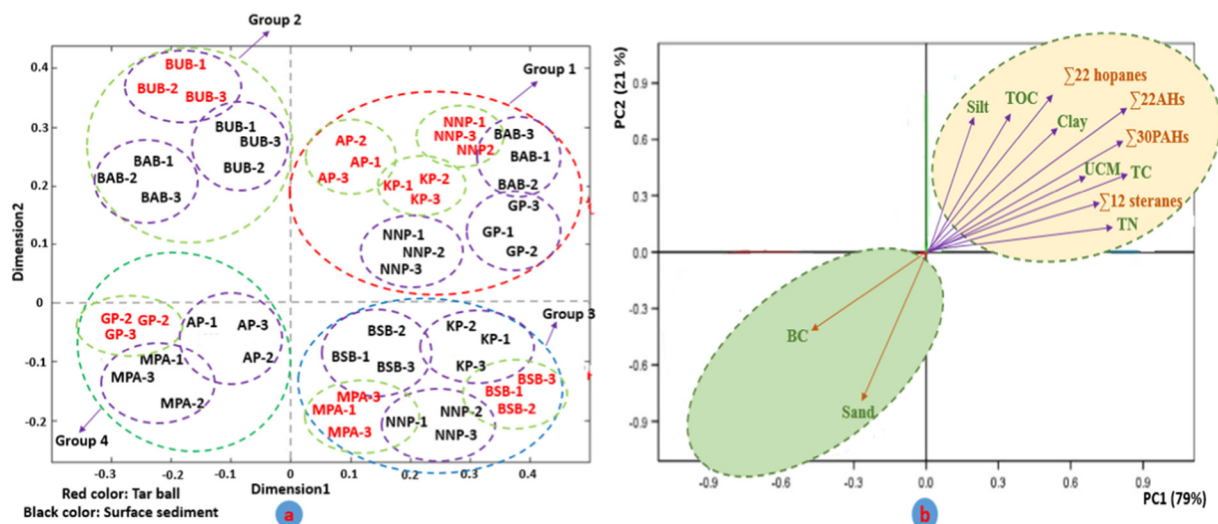


Fig. 7. (a): C<sub>29</sub>/C<sub>30</sub> vs. ΣC<sub>31</sub>-C<sub>35</sub>/C<sub>30</sub> cross-plot diagram for tar ball and oil samples (b): Double ratio plots using biomarkers. C<sub>28</sub> αββ/(C<sub>27</sub> αββ + C<sub>29</sub> αββ) vs. C<sub>29</sub> αββ/(C<sub>27</sub> αββ + C<sub>28</sub> αββ). (c): Results of PCA of the 25 source-specific biomarker parameters versus oil samples from Bahregansar, Soroush, Abuzar and Nowruz oils with tar ball and coastal surface samples.



**Fig. 8.** Loading plot of principal component analysis (PCA) on sampling sites based on total concentration of petroleum pollutants (a) and total *n*-alkanes, PAHs, hopanes, steranes, UCM, TC, TOC, TN, BC, and grain size (clay, silt and sand) in the coastal sediments of the whole study area (b).

**Note:** stations with red color refer to tar balls and black one is for surface sediments.

Additionally, in the whole study to abate the intricate interactions between the biomarkers and bulk parameters (particle size data, TC, TOC and BC) and prepare intuitions into commonalities and discrepancies in the total study area and also between sampling stations, PCA was conducted. The obtained results were plotted in a PCA scatter diagram (Fig. S2). PC<sub>1</sub> elucidated 87% of the total variance. The resultant data also revealed that  $\Sigma_{22}$ AHs, UCM,  $\Sigma_{30}$ PAHs,  $\Sigma_{22}$ hopanes and  $\Sigma_{12}$ steranes elucidated by 71.15% of the total variance from PC<sub>1</sub> (23.60%, 30.15%, and 17.40 respectively), while other bulk physical data accounted for 23.25% of the total variance. Overall, two separate loadings from PCA was determined:  $\Sigma_{22}$ AHs, UCM,  $\Sigma_{30}$ PAHs,  $\Sigma_{22}$ hopanes and  $\Sigma_{12}$ steranes along with value of TC, TOC, TN, clay, and silt are loaded simultaneously toward the top right of the plot, while BC and sand is closely grouped to the top left of plot (Fig. 8b). Variations in concentrations of biomarkers could be interpreted by numerous factors including the affinity of the sampling sites to polluted sources, sediment properties, grain size and as well as TOC (Kucklick et al., 1997; Abdi et al., 2018). It seems that noticeable differences, which were observed for various concentration of petroleum hydrocarbons among various sampling sites, could be due to the discrepancies in particle size of their coastal sediments. Our study revealed that despite significantly strong positive correlation among clay portion of coastal sediments with total biomarkers, all detected biomarkers were not significantly associated with sand sediment type ( $p > 0.05$ ) and were associated by a negative correlation with BC (Fig. 8b) and it is consistent with similar studies in the Persian Gulf, which have reported the relationship between TOC, clay and biomarker concentrations (Ranjbar Jafarabadi et al., 2017a, 2018b; Rostami et al., 2019; Wen et al., 2018; Bernabeu et al., 2013).

To distinguish the individual stations based on concentration of petroleum biomarkers and bulk parameters (TC, TOC, BC, TN, clay, silt and sand), NPMDS was also conducted and the results revealed four groups (Fig. 8a). As can be seen in Fig. 8a, based on the intensity of anthropogenic activities, NPMDS analysis revealed four clusters of sampling sites. Group1 belongs to GP, BAB, NNP, AP and KP with high concentration of *n*-alkanes, PAHs, and petroleum biomarkers (hopanes and steranes), in sediments and tar balls, plus higher values of TC, TOC, clay, and silt, and undergoing extremely anthropogenic effects. Group 2 includes BUB and BAB along with moderate to almost high amounts of petroleum hydrocarbons and undergoing moderate anthropogenic effects. Group 3 belonged to BSB, KP, NNP and MPA with medium concentration of petroleum compounds and as well as dominance of silt. AP, MPA and GP were classified in group 4 with low to medium

concentrations of biomarkers and lower influence of industrial activities. Generally speaking, these findings demonstrate that our study area are impacted by a number of human activities from oil extraction of oil wells (either located in the offshore and onshore) to crude oil processing facilities, and the cross-plot diagram and PCA indicated that the tar ball and coastal sediment samples deposited along the Southwest of the BP beaches in the Persian Gulf during 2014 are most likely originated from the Abuzar oil.

#### 4. Conclusion

We reported the first study of the occurrence, spatial distribution, as well as source apportionment of *n*-alkanes, PAH, hopanes and steranes in coastal sediment and tar ball samples from a matrix of eight coastal ecosystems in the BP, Persian Gulf, Iran. The main consequences of this study were:

- The distribution of TOC correlated strongly with coastal sediment grain size with the clay particles having the highest concentration, suggested the influence of hydrodynamics on the accumulation of organic matters and the C/N ratios revealed different inputs of OM (mostly marine and to some extent terrestrial origins), plausible post-depositional biodegradation and possibly hydrodynamic sorting processes.
- *n*-alkanes, PAH and petroleum biomarker (hopane and sterane) concentrations in this coastal environment varied significantly among sampling locations and two matrices (coastal sediments and tar balls). Similar trend for total hydrocarbons in both matrices was not observed.
- The presence of UCM exhibited the presence of petroleum contamination in the majority of sampling sites, mostly from anthropogenic activities such as offshore and onshore oil exploration and extraction along with shipping.
- PCA analysis revealed that among the congeners of petroleum biomarkers, HMW-*n*-alkanes ( $> n-C_{20}$ ) and UCM for *n*-alkanes, alkylated phenanthrene, BaP, BghiP and perylene for PAHs,  $C_{30}\alpha\beta$  and  $C_{29}\alpha\beta$  for hopanes and 27  $\beta\beta$ S, 27 $\beta\beta$ R, 28  $\beta\beta$ S, and 28 $\beta\beta$ R for steranes, were discriminated from their other congeners in sediments and tar balls, suggesting a combination of petrogenic (more) and pyrolytic sources of organic matters.
- Based on the diagnostic ratios of *n*-alkane, PAHs, hopane, and steranes analysis, it is inferred that the tar balls that were deposited

along the Southwest coast of the Bushehr Province (BP) in 2014 have the features of floating tar balls. The tar ball samples were all noticeably analogous and consistent with the same source. The consequences of source identification by using PCA and cross plot of the diagnostic ratios of Abuzar, Soroush, Bahregansar and Nowruz oil wells prove that the source of the coastal sediment and tar ball samples analyzed is most likely from the Abuzar oil. Further estimation is needed to confirm a definite source for the tar balls.

- Based on the intensity of anthropogenic activities, NPMSD revealed sampling sites of GP, BAB, NNP, AP and KP have high concentration of detected organic pollutants, in sediments and tar balls, plus higher values of TOC, clay, and silt, and undergoing extremely anthropogenic effects.

## Acknowledgement

The support by the National Iranian South Oilfields Company (NISOC) that provided partial funding for this project is highly appreciated.

## Appendix A. Supplementary data

Supplementary data to this article can be found online at <https://doi.org/10.1016/j.marpolbul.2019.07.023>.

## References

- Abdi, E., Babapour, S., Majnoonian, B., Amiri, G.Z., Deljouei, A., 2018. How does organic matter affect the physical and mechanical properties of forest soil? [J]. *J. For. Res.* 29 (3), 657–662.
- Abdollahi, S., Raoufi, Z., Faghiri, I., Savari, A., Nikpour, Y., Mansouri, A., 2013. Contamination levels and spatial distributions of heavy metals and PAHs in surface sediment of Imam Khomeini Port, Persian Gulf, Iran. *Mar. Pollut. Bull.* 71 (1–2), 336–345.
- Aboul-Kassim, T.A., Simoneit, B.R., 1996. Lipid geochemistry of surficial sediments from the coastal environment of Egypt I. Aliphatic hydrocarbons-characterization and sources. *Mar. Chem.* 54 (1–2), 135–158.
- Agah, H., Mehdinia, A., Bastami, K.D., Rahmanpour, S., 2017. Polycyclic aromatic hydrocarbon pollution in the surface water and sediments of Chabahar Bay, Oman Sea. *Mar. Pollut. Bull.* 115 (1–2), 515–524.
- Aghadadashi, V., Mehdinia, A., 2016. Occurrence, spatial deposition and footprint of polybrominated diphenyl ethers in surficial sediments of Bushehr peninsula, the Persian Gulf. *Mar. Pollut. Bull.* 112 (1–2), 211–217.
- Aghadadashi, V., Mehdinia, A., Molaie, S., 2016. Origin, toxicological and narcotic potential of sedimentary PAHs and remarkable even/odd *n*-alkane predominance in Bushehr Peninsula, the Persian Gulf. *Mar. Pollut. Bull.* 114 (1), 494–504.
- Akhbarizadeh, R., Moore, F., Keshavarzi, B., Moeinpour, A., 2016. Aliphatic and polycyclic aromatic hydrocarbons risk assessment in coastal water and sediments of Khark Island, SW Iran. *Mar. Pollut. Bull.* 108 (1–2), 33–45.
- Amir-Heidari, P., Raie, M., 2018. Probabilistic risk assessment of oil spill from offshore oil wells in Persian gulf. *Mar. Pollut. Bull.* 136, 291–299.
- de Andrade Passos, E., Alves, J.C., dos Santos, I.S., Jose do Patrocínio, H.A., Garcia, C.A.B., Costa, A.C.S., 2010. Assessment of trace metals contamination in estuarine sediments using a sequential extraction technique and principal component analysis. *Microchem. J.* 96 (1), 50–57.
- Azimi Yancheshmeh, R., Riyahi Bakhtiari, A.R., Mortazavi, S., 2014. Ecological risk assessment of polycyclic aromatic compounds in the surface sediments of Anzali Wetland in 2010. *Iranian Journal of Health and Environment* 7 (2), 157–170.
- Bacosa, H.P., Thyng, K.M., Plunkett, S., Erdner, D.L., Liu, Z., 2016. The tar balls on Texas beaches following the 2014 Texas City “Y” spill: modeling, chemical, and microbiological studies. *Mar. Pollut. Bull.* 109 (1), 236–244.
- Baumard, P., Budzinski, H., Garrigues, P.H., Sorbe, J.C., Burgeot, T., Bellocq, J., 1998. Concentrations of PAHs (polycyclic aromatic hydrocarbons) in various marine organisms in relation to those in sediments and to trophic level. *Mar. Pollut. Bull.* 36 (12), 951–960.
- Bayona, J.M., Dominguez, C., Albaigés, J., 2015. Analytical developments for oil spill fingerprinting. *Trends in Environmental Analytical Chemistry* 5, 26–34.
- Bemaniharanagh, A., Riyahi Bakhtiari, A., Mohammadi, J., Taghizadeh-Mehrjardi, R., 2017. Characterization and ecological risk of polycyclic aromatic hydrocarbons (PAHs) and *n*-alkanes in sediments of Shadegan international wetland, the Persian Gulf. *Mar. Pollut. Bull.* 124 (1), 155–170.
- Bernabeu, A.M., Fernández-Fernández, S., Bouchette, F., Rey, D., Arcos, A., Bayona, J.M., Albaigés, J., 2013. Recurrent arrival of oil to Galician coast: the final step of the prestige deep oil spill. *J. Hazard. Mater.* 250–251, 82–90.
- Bouloubassi, I., Fillaux, J., Saliot, A., 2001. Hydrocarbons in surface sediments from the Changjiang (Yangtze River) estuary, East China Sea. *Mar. Pollut. Bull.* 42 (12), 1335–1346.
- Brassell, S.C., Gowar, A.P., Eglinton, G., 1980. Computerised gas chromatography-mass spectrometry in analyses of sediments from the Deep Sea drilling project. *Phys. Chem. Earth* 12, 421–426.
- Budzinski, H., Jones, I., Bellocq, J., Pierard, C., Garrigues, P.H., 1997. Evaluation of sediment contamination by polycyclic aromatic hydrocarbons in the Gironde estuary. *Mar. Chem.* 58 (1–2), 85–97.
- Burt, J., 2014. The environmental costs of coastal urbanization in the Arabian Gulf. In: *City: analysis of urban trends, culture, theory, policy, action*. 18. pp. 760–770. <https://www.tandfonline.com/doi/abs/10.1080/13604813.2014.962889>.
- Burton, G.A., Johnston, E.L., 2010. Assessing contaminated sediments in the context of multiple stressors. *Environ. Toxicol. Chem.* 29 (12), 2625–2643.
- Butler, J.N., Wells, P.J., Johnson, S., Manock, J.J., 1998. Beach tar on Bermuda: recent observations and implications for global monitoring. *Mar. Pollut. Bull.* 36 (6), 458–463.
- Cabral, A.C., Stark, J.S., Kolm, H.E., Martins, C.C., 2018. An integrated evaluation of some faecal indicator bacteria (FIB) and chemical markers as potential tools for monitoring sewage contamination in subtropical estuaries. *Environ. Pollut.* 235, 739–749.
- Carstensen, J., Klais, R., Cloern, J.E., 2015. Phytoplankton blooms in estuarine and coastal waters: seasonal patterns and key species. *Estuar. Coast. Shelf Sci.* 162, 98–109.
- Chen, C.Y., Chen, F.A., Wu, A.B., Hsu, H.C., Kang, J.J., Cheng, H.W., 1996. Effect of hydroxypropyl- $\beta$ -cyclodextrin on the solubility, photostability and in-vitro permeability of alkannin/shikonin enantiomers. *Int. J. Pharm.* 141 (1–2), 171–178.
- Colombo, J.C., Barreda, A., Bilos, C., Cappelletti, N., Migoya, M.C., Skorupka, C., 2005. Oil spill in the Río de la Plata estuary, Argentina: 2-hydrocarbon disappearance rates in sediments and soils. *Environ. Pollut.* 134 (2), 267–276.
- Commendatore, M.G., Esteves, J.L., Colombo, J.C., 2000. Hydrocarbons in coastal sediments of Patagonia, Argentina: levels and probable sources. *Mar. Pollut. Bull.* 40 (11), 989–998.
- Commendatore, M.G., Nievas, M.L., Amin, O., Esteves, J.L., 2012. Sources and distribution of aliphatic and polyaromatic hydrocarbons in coastal sediments from the Ushuaia Bay (Tierra del Fuego, Patagonia, Argentina). *Mar. Environ. Res.* 74, 20–31.
- Cripps, G.C., 1989. Problems in the identification of anthropogenic hydrocarbons against natural background levels in the Antarctic. *Antarct. Sci.* 1 (4), 307–312.
- Dauner, A.L., Dias, T.H., Ishii, F.K., Libardoni, B.G., Parizzi, R.A., Martins, C.C., 2018. Ecological risk assessment of sedimentary hydrocarbons in a subtropical estuary as tools to select priority areas for environmental management. *J. Environ. Manag.* 223, 417–425.
- Derrien, M., Yang, L., Hur, J., 2017. Lipid biomarkers and spectroscopic indices for identifying organic matter sources in aquatic environments: a review. *Water Res.* 112, 58–71.
- Dietrich, M.A., Arnold, G.J., Fröhlich, T., Ciereszko, A., 2014. In-depth proteomic analysis of carp (*Cyprinus carpio* L.) spermatozoa. *Comparative Biochemistry and Physiology Part D: Genomics and Proteomics* 12, 10–15.
- Dudhagara, D.R., Rajpara, R.K., Bhatt, J.K., Gosai, H.B., Sachaniya, B.K., Dave, B.P., 2016. Distribution, sources and ecological risk assessment of PAHs in historically contaminated surface sediments at Bhavnagar coast, Gujarat, India. *Environ. Pollut.* 213, 338–346.
- Duong, H.T., Kadokami, K., Pan, S., Matsuura, N., Nguyen, T.Q., 2014. Screening and analysis of 940 organic micro-pollutants in river sediments in Vietnam using an automated identification and quantification database system for GC-MS. *Chemosphere* 107, 462–472.
- Dvorská, A., Lammel, G., Klánová, J., 2011. Use of diagnostic ratios for studying source apportionment and reactivity of ambient polycyclic aromatic hydrocarbons over Central Europe. *Atmos. Environ.* 45 (2), 420–427.
- Fu, J., Guoying, S., 1989. Biological marker composition of typical source rocks and related crude oils of terrestrial origin in the People's Republic of China: a review. *Appl. Geochem.* 4 (1), 13–22.
- Gao, X., Chen, S., Xie, X., Long, A., Ma, F., 2007. Non-aromatic hydrocarbons in surface sediments near the Pearl River estuary in the South China Sea. *Environ. Pollut.* 148 (1), 40–47.
- Gogou, A., Bouloubassi, I., Stephanou, E.G., 2000. Marine organic geochemistry of the Eastern Mediterranean: 1. Aliphatic and polyaromatic hydrocarbons in Cretan Sea surficial sediments. *Mar. Chem.* 68 (4), 265–282.
- Gomez-Belinchon, J.I., Grimalt, J.O., Albaigés, J., 1988. Intercomparison study of liquid-liquid extraction and adsorption on polyurethane and Amberlite XAD-2 for the analysis of hydrocarbons, polychlorobiphenyls, and fatty acids dissolved in seawater. *Environmental Science & Technology* 22 (6), 677–685.
- Gough, M.A., Rowland, S.J., 1990. Characterization of unresolved complex mixtures of hydrocarbons in petroleum. *Nature* 344, 648–650.
- Grimalt, J., Albaigés, J., 1987. Sources and occurrence of C12 C22 *n*-alkane distributions with even carbon-number preference in sedimentary environments. *Geochim. Cosmochim. Acta* 51 (6), 1379–1384.
- Guitart, C., García-Flor, N., Bayona, J.M., Albaigés, J., 2007. Occurrence and fate of polycyclic aromatic hydrocarbons in the coastal surface microlayer. *Mar. Pollut. Bull.* 54 (2), 186–194.
- Hammer, Ø., Harper, D., Ryan, P., 2001. PAST: paleontological statistics software package for education and data analysis. *Palaentologia Electron* 4 (1), 1–9.
- Harris, K.A., Yunker, M.B., Dangerfield, N., Ross, P.S., 2011. Sediment-associated aliphatic and aromatic hydrocarbons in coastal British Columbia, Canada: concentrations, composition, and associated risks to protected sea otters. *Environ. Pollut.* 159 (10), 2665–2674.
- Hassanshahian, M., Emtiazi, G., Caruso, G., Cappello, S., 2014. Bioremediation (bioaugmentation/biostimulation) trials of oil polluted seawater: a mesocosm simulation study. *Mar. Environ. Res.* 95, 28–38.
- Hayworth, J.S., Clement, T.P., Valentine, J.F., 2011. Deepwater Horizon oil spill impacts on Alabama beaches. *Hydrology & Earth System Sciences* 15 (12).
- He, D., Zhang, K., Cui, X., Tang, J., Suna, Y., 2018. Spatiotemporal variability of hydrocarbons in surface sediments from an intensively human-impacted Xiaoqing River-Laizhou Bay system in the eastern China: occurrence, compositional profile and source apportionment. *Sci. Total Environ.* 645, 1172–1182.
- Hostettler, F.D., Rosenbauer, R.J., Lorenson, T.D., Dougherty, J., 2004. Geochemical

- characterization of tar balls on beaches along the California coast. Part I-shallow seepage impacting the Santa Barbara Channel Islands, Santa Cruz, Santa Rosa and San Miguel. *Org. Geochem.* 35 (6), 725–746.
- Hu, L., Guo, Z., Feng, J., Yang, Z., Fang, M., 2009. Distributions and sources of bulk organic matter and aliphatic hydrocarbons in surface sediments of the Bohai Sea, China. *Mar. Chem.* 113 (3–4), 197–211.
- Huang, Q., Mao, F., Han, X., Yan, J., Chi, Y., 2014. Characterization of emulsified water in petroleum sludge. *Fuel* 118, 214–219.
- Hughes, W.B., Holba, A.G., Dzou, L.L., 1995. The ratios of dibenzothiophene to phenanthrene and pristane to phytane as indicators of depositional environment and lithology of petroleum source rocks. *Geochim. Cosmochim. Acta* 59 (17), 3581–3598.
- Islam, M.S., Tanaka, M., 2004. Impacts of pollution on coastal and marine ecosystems including coastal and marine fisheries and approach for management: a review and synthesis. *Mar. Pollut. Bull.* 48 (7–8), 624–649.
- Ismail, A., Toriman, M.E., Juahir, H., Kassim, A.M., Zain, S.M., Ahmad, W.K.W., Wong, K.F., Retnam, A., Zali, M.A., Mokhtar, M., Yusri, M.A., 2016. Chemometric techniques in oil classification from oil spill fingerprinting. *Mar. Pollut. Bull.* 111 (1–2), 339–346.
- Jacquot, F., Le Dréau, Y., Doumenq, P., Munoz, D., Guiliano, M., Imbert, G., Mille, G., 1999. The origins of hydrocarbons trapped in the lake of Berre sediments. *Chemosphere* 39 (9), 1407–1419.
- Jeng, W.L., 2007. Aliphatic hydrocarbon concentrations in short sediment cores from the southern Okinawa Trough: implications for lipid deposition in a complex environment. *Cont. Shelf Res.* 27 (15), 2066–2078.
- Kalaitzoglou, M., Terzi, E., Samara, C., 2004. Patterns and sources of particle-phase aliphatic and polycyclic aromatic hydrocarbons in urban and rural sites of western Greece. *Atmos. Environ.* 38 (16), 2545–2560.
- Kao, N.H., Su, M.C., Fan, J.R., Chung, Y.Y., 2015. Identification and quantification of biomarkers and polycyclic aromatic hydrocarbons (PAHs) in an aged mixed contaminated site: from source to soil. *Environ. Sci. Pollut. Res.* 22 (10), 7529–7546.
- Keshavarzifard, M., Moore, F., Keshavarzi, B., Sharifi, R., 2017. Polycyclic aromatic hydrocarbons (PAHs) in sediment and sea urchin (*Echinometra mathaei*) from the intertidal ecosystem of the northern Persian Gulf: distribution, sources, and bioavailability. *Mar. Pollut. Bull.* 123 (1–2), 373–380.
- Khaksar, F., Nejatkhah Manavi, P., Ashja Ardalan, A., Abedi, A., Saleh, A., 2019. Concentration of polycyclic aromatic hydrocarbons in zooplanktons of Bushehr coastal waters (north of the Persian Gulf). *Mar. Pollut. Bull.* 140, 35–39.
- Khan, N.Y., 2002. *Physical and Human Geography*, chapter. 1. In: *The Gulf Ecosystem: Health and Sustainability*. Backhuys Publishers, Leiden, the Netherlands.
- Khazaali, A., Kunzmann, A., Bastami, K.D., Baniamam, M., 2015. Baseline of polycyclic aromatic hydrocarbons in the surface sediment and sea cucumbers (*Holothuria leucospilota* and *Stichopus hermanni*) in the northern parts of Persian Gulf. *Mar. Pollut. Bull.* 110 (1), 539–545.
- Kim, K.H., Jahan, S.A., Kabir, E., Brown, R.J., 2013. A review of airborne polycyclic aromatic hydrocarbons (PAHs) and their human health effects. *Environ. Int.* 60, 71–80.
- Kirman, Z.D., Sericano, J.L., Wade, T.L., Bianchi, T.S., Marcantonio, F., Kolker, A.S., 2016. Composition and depth distribution of hydrocarbons in Barataria Bay marsh sediments after the Deepwater horizon oil spill. *Environ. Pollut.* 214, 101–113.
- Kostka, J.E., Prakash, O., Overholt, W.A., Green, S., Freyer, G., Canion, A., Delgado, J., Norton, N., Hazen, T.C., Huettel, M., 2011. Hydrocarbon-degrading bacteria and the bacterial community response in Gulf of Mexico beach sands impacted by the Deepwater Horizon oil spill. *Appl. Environ. Microbiol.* 77 (22), 7962–7974.
- Kucklick, J.R., Sivertsen, S.K., Sanders, M., Scott, G.I., 1997. Factors influencing polycyclic aromatic hydrocarbon distributions in South Carolina estuarine sediments. *J. Exp. Mar. Biol. Ecol.* 213 (1), 13–29.
- Kvenvolden, K.A., Rosenbauer, R.J., Hostettler, F.D., Lorenson, T.D., 2000. Application of organic geochemistry to coastal tar residues from central California. *Int. Geol. Rev.* 42 (1), 1–14.
- Lamine, S., Xiong, D., 2013. Guinean environmental impact potential risks assessment of oil spills simulation. *Ocean Eng.* 66, 44–57.
- Li, J., Yang, D., Li, L., Jabene, K., Shi, H., 2015. Microplastics in commercial bivalves from China. *Environ. Pollut.* 207, 190–195.
- Lima, M.B., Feitosa, E.A., Emídio, E.S., Dórea, H.S., Alexandre, M.R., 2012. Distribution and sources of aliphatic hydrocarbons in surface sediments of Sergipe River estuarine system. *Mar. Pollut. Bull.* 64 (8), 1721–1725.
- Liu, Y., Chen, L., Huang, Q.H., Li, W.Y., Tang, Y.J., Zhao, J.F., 2009. Source apportionment of polycyclic aromatic hydrocarbons (PAHs) in surface sediments of the Huangpu River, Shanghai, China. *Sci. Total Environ.* 407 (8), 2931–2938.
- Liu, L.Y., Wang, J.Z., Wei, G.L., Guan, Y.F., Zeng, E.Y., 2012. Polycyclic aromatic hydrocarbons (PAHs) in continental shelf sediment of China: implications for anthropogenic influences on coastal marine environment. *Environ. Pollut.* 167, 155–162.
- Liu, P.W.G., Chang, T.C., Chen, C.H., Wang, M.Z., Hsu, H.W., 2014. Bioaugmentation efficiency investigation on soil organic matters and microbial community shift of diesel-contaminated soils. *Int. Biodeterior. Biodegradation* 95 (A), 276–284.
- Louati, A., Elleuch, B., Kallel, M., Saliot, A., Dagaut, J., Odout, J., 2001. Hydrocarbon contamination of coastal sediments from the Sfax area (Tunisia), Mediterranean Sea. *Mar. Pollut. Bull.* 42 (6), 444–451.
- Maciel, D.C., de Souza, J.R.B., Taniguchi, S., Bicego, M.C., Schettini, C.A.F., Zanardi-Lamardo, E., 2016. Hydrocarbons in sediments along a tropical estuary-shelf transition area: sources and spatial distribution. *Mar. Pollut. Bull.* 113 (1–2), 566–571.
- Mackenzie, I.C., 1984. The role of epithelial-mesenchymal interactions in epithelial migration and differentiation. *J. Periodontol Res.* 19 (6), 656–660.
- Manan, N., Raza, M., Yuh, Y.S., Theng, L.W., Zakaria, M.P., 2011. Distribution of petroleum hydrocarbons in aquaculture fish from selected locations in the straits of Malacca, Malaysia. *World Appl. Sci. J.* 14, 14–21.
- Martinez-Silva, M.A., Audet, C., Winkler, G., Tremblay, R., 2018. Prey quality impact on the feeding behavior and lipid composition of winter flounder (*Pseudopleuronectes americanus*) larvae[J]. *Aquaculture and Fisheries* 3 (4), 145–155.
- Martins, M., Santos, J.M., Diniz, M.S., Ferreira, A.M., Costa, M.H., Costa, P.M., 2015. Effects of carcinogenic versus non-carcinogenic AHR-active PAHs and their mixtures: lessons from ecological relevance. *Environ. Res.* 138, 101–111.
- Medeiros, P.M., Bicego, M.C., Castela, R.M., Del Rosso, C., Fillmann, G., Zamboni, A.J., 2005. Natural and anthropogenic hydrocarbon inputs to sediments of Patos Lagoon Estuary, Brazil. *Environ. Int.* 31 (1), 77–87.
- Mehdini, A., Aghadadashi, V., Shejoooni Fumani, N., 2015. Origin, distribution and toxicological potential of polycyclic aromatic hydrocarbons in surface sediments from the Bushehr coast, The Persian Gulf. *Mar. Pollut. Bull.* 90 (1–2), 334–338.
- Meyers, P.A., 2003. Applications of organic geochemistry to paleolimnological reconstructions: a summary of examples from the Laurentian Great Lakes. *Org. Geochem.* 34 (2), 261–289.
- Michel, J., Owens, E.H., Zengel, S., Graham, A., Nixon, Z., Allard, T., Holton, W., Reimer, P.D., Lamarche, A., White, M., Rutherford, N., Childs, C., Mauseth, G., Challenger, G., Taylor, E., 2013. Extent and degree of shoreline oiling: Deepwater Horizon oil spill, Gulf of Mexico, USA. *PLoS One* 8 (6), 1–9 e65087.
- Mille, G., Asia, L., Guiliano, M., Malleret, L., Doumenq, P., 2007. Hydrocarbons in coastal sediments from the Mediterranean Sea (Gulf of Fos area, France). *Mar. Pollut. Bull.* 54 (5), 566–575.
- Mohebbi-Nozar, S.L., Zakaria, M.P., Ismail, W.R., Mortazawi, M.S., Salimizadeh, M., Momeni, M., Akbarzadeh, G., 2015. Total petroleum hydrocarbons in sediments from the coastline and mangroves of the northern Persian Gulf. *Mar. Pollut. Bull.* 95 (1), 407–411.
- Mokhtari, M., Ghaffar, M.A., Usup, G., Cob, Z.C., 2015. Determination of key environmental factors responsible for distribution patterns of fiddler crabs in a tropical mangrove ecosystem. *PLoS One* 10 (1), 1–17 e0117467.
- Niamainandi, N., Javadzadeh, N., Kabgani, N., Ghorbani Vaghei, R., Rajabzadeh, I., 2017. Biodiversity of the gastropods in different periods in intertidal zone of the Iranian waters of the Persian Gulf. *Reg. Stud. Mar. Sci.* 13, 59–63.
- Nkem, B.M., Halimoon, N., Yusoff, F.M., Johari, W.L.W., Zakaria, M.P., Medipally, S.R., Kannan, N., 2016. Isolation, identification and diesel-oil biodegradation capacities of indigenous hydrocarbon-degrading strains of *Cellulosimicrobium cellulans* and *Acinetobacter baumannii* from tar ball at Terengganu beach, Malaysia. *Mar. Pollut. Bull.* 107 (1), 261–268.
- Noroozi Karbasdehi, V., Dobaradaran, S., Nabipour, I., Ostovar, A., Arfaeinia, H., Vazirizadeh, A., Mirahmadi, R., Keshkar, M., Faraji Ghasemi, F., Khalifei, F., 2017. Indicator bacteria community in seawater and coastal sediment: the Persian Gulf as a case. *Journal of Environmental Health Science & Engineering* 15 (6), 1–17.
- OSAT-2 (Operational Science Advisory Team-2), 2011. *Summary Report for Fate and Effects of Remnant Oil in the Beach Environment*. (February 10). (TREX-012238). Prepared for Capt. Lincoln D. Stroh, U.S. Coast Guard, Federal on-Scene Coordinator, Deepwater Horizon MC252. Retrieved from: [http://www.dep.state.fl.us/deepwaterhorizon/files2/osat\\_2\\_report\\_10feb.pdf](http://www.dep.state.fl.us/deepwaterhorizon/files2/osat_2_report_10feb.pdf).
- OSAT-3 (Operational Science Advisory Team-3), 2013. *Investigation of Recurring Residual Oil in Discrete Shoreline Areas in the Eastern Area of Responsibility*. (October). (TREX-011826). Prepared for Capt. Thomas Sparks, U.S. Coast Guard Federal on-Scene Coordinator, Deepwater Horizon MC252. Retrieved from: <https://www.restorethegulf.gov/sites/default/files/u372/OSAT%20III%20Eastern%20States.pdf>.
- Ou, S., Zheng, J., Zheng, J., Richardson, B.J., Lam, P.K.S., 2004. Petroleum hydrocarbons and polycyclic aromatic hydrocarbons in the surficial sediments of Xiamen Harbour and Yuan Dan Lake, China. *Chemosphere* 56 (2), 107–112.
- Pang, X., Li, M., Li, S., Jina, Z., 2003. Geochemistry of petroleum systems in the Niuzhuang South Slope of Bohai Bay Basin. Part 2: evidence for significant contribution of mature source rocks to “immature oils” in the Bamiandhe field. *Org. Geochem.* 34 (7), 931–950.
- Parlanti, E., 1990. Utilisation des hydrocarbures comme traceurs d'origine et d'évolution de la matière organique sédimentaire en milieu marin. Etude du Golfe du Lion et du Golfe de Gascogne: programme ECOMARGE (Doctoral dissertation). University of Bordeaux 1, Bordeaux, France.
- Pavlova, A., Papazova, D., 2003. Oil-spill identification by gas chromatography-mass spectrometry. *J. Chromatogr. Sci.* 41 (5), 271–273.
- Pearson, A., Eglinton, T.I., 2000. The origin of n-alkanes in Santa Monica Basin surface sediment: a model based on compound-specific  $\Delta^{14}C$  and  $\delta^{13}C$  data. *Org. Geochem.* 31 (11), 1103–1116.
- Perelo, L.W., 2010. In situ and bioremediation of organic pollutants in aquatic sediments. *J. Hazard. Mater.* 177 (1–3), 81–89.
- Peters, K.E., Moldovan, J.M., 1993. *The Biomarker Guide: Interpreting Molecular Fossils in Petroleum and Ancient Sediments*. Prentice Hall, Englewood Cliffs, New Jersey, United States.
- Peters, K.E., Walters, C.C., Moldovan, J.M., 2005. *The Biomarker Guide*, 2nd edition. Biomarkers and Isotopes in the Environment and Human History 1 Cambridge University Press, New York, United States.
- Prahl, F.G., Carpenter, R., 1983. Polycyclic aromatic hydrocarbon (PAH)-phase associations in Washington coastal sediment. *Geochim. Cosmochim. Acta* 47 (6), 1013–1023.
- Rahmanpoor, S., Ghafourian, H., Hashtroudi, S.M., Darvish Bastami, K., 2013. Distribution and sources of polycyclic aromatic hydrocarbons in surface sediments of the Hormuz strait, Persian Gulf. *Mar. Pollut. Bull.* 78 (1–2), 224–229.
- Ramsey, E., Meyer, B.M., Ragoonwala, A., Overton, E., Jones, C.A., Bannister, T., 2014. Oil source-fingerprinting in support of polarimeter radar mapping of Macondo-252 oil in Gulf Coast marshes. *Mar. Pollut. Bull.* 89 (1–2), 85–95.
- Ranjbar Jafarabadi, A., Riyahi Bakhtiari, A., Aliabadian, M., Shadmehri Toosi, A., 2017a. Spatial distribution and composition of aliphatic hydrocarbons, polycyclic aromatic hydrocarbons and hopanes in superficial sediments of the coral reefs of the Persian Gulf, Iran. *Environ. Pollut.* 224, 195–223.
- Ranjbar Jafarabadi, A., Riyahi Bakhtiari, A., Shadmehri Toosi, A., Jadot, C., 2017b. Spatial distribution, ecological and health risk assessment of heavy metals in marine surface sediments and coastal seawaters of fringing coral reefs of the Persian Gulf, Iran. *Chemosphere* 185, 1090–1111.
- Ranjbar Jafarabadi, A., Riyahi Bakhtiari, A., Shadmehri Toosi, A., 2017c. Comprehensive

- and comparative ecotoxicological and human risk assessment of polycyclic aromatic hydrocarbons (PAHs) in reef surface sediments and coastal seawaters of Iranian Coral Islands, Persian Gulf. *Ecotoxicol. Environ. Saf.* 145, 640–652.
- Ranjbar Jafarabadi, A., Riyahi Bakhtiari, A., Maisano, M., Pereira, P., Cappello, T., 2018a. First record of bioaccumulation and bioconcentration of metals in Scleractinian corals and their algal symbionts from Kharg and Lark coral reefs (Persian Gulf, Iran). *Sci. Total Environ.* 640–641, 1500–1511.
- Ranjbar Jafarabadi, A., Riyahi Bakhtiari, A., Aliabadian, M., Hedouin, L., Shadmehri Toosi, A., Yap, C.K., 2018b. First report of bioaccumulation and bioconcentration of aliphatic hydrocarbons (AHs) and persistent organic pollutants (PAHs, PCBs and PCNs) and their effects on alcyonacea and scleractinian corals and their endosymbiotic algae from the Persian Gulf, Iran: inter and intra-species differences. *Sci. Total Environ.* 627, 141–157.
- Ranjbar Jafarabadi, A., Dashtbozorg, M., Riyahi Bakhtiari, A., Maisano, M., Cappello, T., 2019a. Geochemical imprints of occurrence, vertical distribution and sources of aliphatic hydrocarbons, aliphatic ketones, hopanes and steranes in sediment cores from ten Iranian Coral Islands, Persian Gulf. *Mar. Pollut. Bull.* 144, 287–298.
- Jafarabadi, A., Riyahi Bakhtiari, A., Mitra, S., Maisano, M., Cappello, T., Jadot, C., 2019b. First polychlorinated biphenyls (PCBs) monitoring in seawater, surface sediments and marine fish communities of the Persian Gulf: Distribution, levels, congener profile and health risk assessment. 253, 78–88.
- Ray, R., Majumder, N., Das, S., Chowdhury, C., Jana, T.K., 2014. Biogeochemical cycle of nitrogen in a tropical mangrove ecosystem, east coast of India. *Mar. Chem.* 167, 33–43.
- Resmi, P., Manju, M.N., Gireeshkumar, T.R., Kumar, C.R., Chandramohanakumar, N., 2016. Source characterisation of sedimentary organic matter in mangrove ecosystems of northern Kerala, India: inferences from bulk characterisation and hydrocarbon biomarkers. *Reg. Stud. Mar. Sci.* 7, 43–54.
- Riyahi Bakhtiari, A., Zakaria, M.P., Yaziz, M.I., Lajis, M.N.H., Bi, X., Rahim, M.C.A., 2009. Vertical distribution and source identification of polycyclic aromatic hydrocarbons in anoxic sediment cores of Chini Lake, Malaysia: perylene as indicator of land plant-derived hydrocarbons. *Appl. Geochem.* 24 (9), 1777–1787.
- Riyahi Bakhtiari, A., Zakaria, M.P., Yaziz, M.I., Lajis, M.N.H., Bi, X., Shafiee, M.M., Sakari, M., 2010. Distribution of PAHs and *n*-alkanes in Klang River surface sediments, Malaysia. *Pertanika Journal of Science and Technology* 18 (1), 167–179.
- Rostami, S., Abessi, O., Amini-Rad, H., 2019. Assessment of the toxicity, origin, biodegradation and weathering extent of petroleum hydrocarbons in surface sediments of pars special economic energy Zone, Persian Gulf. *Mar. Pollut. Bull.* 138, 302–311.
- Sammarco, P.W., Kolian, S.R., Warby, R.A., Bouldin, J.L., Subra, W.A., Porter, S.A., 2013. Distribution and concentrations of petroleum hydrocarbons associated with the BP/Deepwater Horizon Oil Spill, Gulf of Mexico. *Mar. Pollut. Bull.* 73 (1), 129–143.
- Santos, C.F., Michel, J., Neves, M., Janeiro, J., Andrade, F., Orbach, M., 2013. Marine spatial planning and oil spill risk analysis: finding common grounds. *Mar. Pollut. Bull.* 74 (1), 73–81.
- Shirneshan, G., Riyahi Bakhtiari, A., Memariani, M., 2016. Identification of sources of tar balls deposited along the Southwest Caspian Coast, Iran using fingerprinting techniques. *Sci. Total Environ.* 568, 979–989.
- Shirneshan, G., Riyahi Bakhtiari, A., Memariani, M., 2017. Identifying the source of petroleum pollution in sediment cores of southwest of the Caspian Sea using chemical fingerprinting of aliphatic and alicyclic hydrocarbons. *Mar. Pollut. Bull.* 115 (1–2), 383–390.
- Sicre, M.A., Marty, J.C., Saliot, A., Aparicio, X., Grimalt, J., Albaiges, J., 1987. Aliphatic and aromatic hydrocarbons in different sized aerosols over the Mediterranean Sea: occurrence and origin. *Atmos. Environ.* 21 (10), 2247–2259.
- Simoneit, B.R., 1989. Organic matter of the troposphere-V: application of molecular marker analysis to biogenic emissions into the troposphere for source reconciliations. *J. Atmos. Chem.* 8 (3), 251–275.
- Simoneit, B.R., Mazurek, M.A., 1982. Organic matter of the troposphere-II. Natural background of biogenic lipid matter in aerosols over the rural western United States. *Atmos. Environ.* 16 (9), 2139–2159.
- Singran, N., 2013. Classifying risk zones by the impacts of oil spills in the coastal waters of Thailand. *Mar. Pollut. Bull.* 70 (1–2), 34–43.
- Soclo, H.H., 1986. Etude de la distribution des hydrocarbures aromatiques polycycliques (HAP) dans les sédiments récents. Identification des sources (Doctoral dissertation). University of Bordeaux 1, Bordeaux, France.
- Soclo, H.H., Garrigues, P.H., Ewald, M., 2000. Origin of polycyclic aromatic hydrocarbons (PAHs) in coastal marine sediments: case studies in Cotonou (Benin) and Aquitaine (France) areas. *Mar. Pollut. Bull.* 40 (5), 387–396.
- de Souza Neto, E.A., Peric, D., Owen, D.R., 2008. Computational Methods for Plasticity: Theory and Applications. John Wiley & Sons, Hoboken, United States.
- Suneel, V., Vethamony, P., Naik, B.G., Kumar, K.V., Sreenu, L., Samiksha, S.V., Tai, Y., Sudheesh, K., 2014. Source investigation of the tar balls deposited along the Gujarat coast, India, using chemical fingerprinting and transport modeling techniques. *Environmental Science & Technology* 48 (19), 11343–11351.
- Takada, H., Eganhouse, R.P., 1998. Molecular markers of anthropogenic waste. In: Meyers, R.A. (Ed.), *Encyclopedia of Environmental Analysis and Remediation*. John Wiley & Sons, Hoboken, United States, pp. 2883–2940 Inc.
- Tolosa, I., de Mora, S.J., Fowler, S.W., Villeneuve, J., Bartocci, J., Cattini, C., 2005. Aliphatic and aromatic hydrocarbons in marine biota and coastal sediments from the Gulf and the Gulf of Oman. *Mar. Pollut. Bull.* 50 (12), 1619–1633.
- Vaezzadeh, V., Zakaria, M.P., Bong, C.W., 2017. Aliphatic hydrocarbons and triterpane biomarkers in mangrove oyster (*Crassostrea belcheri*) from the west coast of Peninsular Malaysia. *Mar. Pollut. Bull.* 124 (1), 33–42.
- Varnosfaderany, M.N., Riyahi Bakhtiari, A., Gu, Z., Chu, G., 2014. Vertical distribution and source identification of polycyclic aromatic hydrocarbons (PAHs) in southwest of the Caspian Sea: Most petrogenic events during the late Little Ice Age. *Mar. Pollut. Bull.* 87 (1–2), 152–163.
- Vaughan, G.O., Al-Mansoori, N., Burt, J., 2019. *The Arabian Gulf*. In: Sheppard, C. (Ed.), *World Seas: An Environmental Evaluation*, second edition. Elsevier Science, Amsterdam, NL, pp. 1–23. <https://www.sciencedirect.com/science/article/pii/B9780081008539000014>.
- Volkman, J.K., 2005. Lipid Markers for Marine Organic Matter. *Marine organic matter: Biomarkers, isotopes and DNA*. Springer, Berlin, pp. 27–70.
- Volkman, J.K., Holdsworth, D.G., Neill, G.P., Bavor Jr., H.J., 1992. Identification of natural, anthropogenic and petroleum hydrocarbons in aquatic sediments. *Sci. Total Environ.* 112 (2–3), 203–219.
- Wang, Z., Fingas, M.F., 2003. Development of oil hydrocarbon fingerprinting and identification techniques. *Mar. Pollut. Bull.* 47 (9–12), 423–452.
- Wang, Z., Stout, S.A., Fingas, M., 2006. Forensic fingerprinting of biomarkers for oil spill characterization and source identification. *Environ. Forensic* 7 (2), 105–146.
- Wang, Z., Yang, C., Kelly-Hooper, F., Hollebone, B.P., Peng, X., Brown, C.E., Landriault, M., Sun, J., Yang, Z., 2009. Forensic differentiation of biogenic organic compounds from petroleum hydrocarbons in biogenic and petrogenic compounds cross-contaminated soils and sediments. *J. Chromatogr. A* 1216 (7), 1174–1191.
- Wang, Z., Yang, C., Yang, Z., Sun, J., Hollebone, B., Brown, C., Landriault, M., 2011. Forensic fingerprinting and source identification of the 2009 Sarnia (Ontario) oil spill. *J. Environ. Monit.* 13 (11), 3004–3017.
- Wang, Y.H., Yang, H., Chen, X., Zhang, J.X., Ou, J., Xie, B., Huang, C.C., 2013. Molecular biomarkers for sources of organic matter in lacustrine sediments in a subtropical lake in China. *Environ. Pollut.* 176, 284–291.
- Wang, M., Wang, C., Hu, X., Zhang, H., He, S., Lv, S., 2015. Distributions and sources of petroleum, aliphatic hydrocarbons and polycyclic aromatic hydrocarbons (PAHs) in surface sediments from Bohai Bay and its adjacent river, China. *Mar. Pollut. Bull.* 90 (1–2), 88–94.
- Warnock, A.M., Hagen, S.C., Passeri, D.L., 2015. Marine tar residues: a review. *Water Air Soil Pollut.* 226 (3), 68.
- Wen, B., Chen, Z., Qu, H., Gao, J., 2018. Growth and fatty acid composition of discus fish *Symphysodon haraldi* given varying feed ratios of beef heart, duck heart, and shrimp meat [J]. *Aquaculture and Fisheries* 3 (2), 84–89.
- Wu, Y., Yang, L., Zheng, X., Zhang, S., Song, S., Li, J., Hao, J., 2014. Characterization and source apportionment of particulate PAHs in the roadside environment in Beijing. *Sci. Total Environ.* 470, 76–83.
- Yang, C., Wang, Z., Hollebone, B.P., Brown, C.E., Landriault, M., 2009. Characteristics of bicyclic sesquiterpanes in crude oils and petroleum products. *J. Chromatogr. A* 1216 (20), 4475–4484.
- Yim, U.H., Ha, S.Y., An, J.G., Won, J.H., Han, G.M., Hong, S.H., Kim, M., Jung, J., Shim, W.J., 2011. Fingerprint and weathering characteristics of stranded oils after the Hebei Spirit oil spill. *J. Hazard. Mater.* 197, 60–69.
- Yin, F., John, G.F., Hayworth, J.S., Clement, T.P., 2015. Long-term monitoring data to describe the fate of polycyclic aromatic hydrocarbons in Deepwater Horizon oil submerged off Alabama's beaches. *Sci. Total Environ.* 508, 46–56.
- Yunker, M.B., Macdonald, R.W., 2003. Alkane and PAH depositional history, sources and fluxes in sediments from the Fraser River Basin and Strait of Georgia, Canada. *Org. Geochem.* 34 (10), 1429–1454.
- Yunker, M.B., Backus, S.M., Pannatier, E.G., Jeffries, D.S., Macdonald, R.W., 2002a. Sources and significance of alkane and PAH hydrocarbons in Canadian arctic rivers. *Estuar. Coast. Shelf Sci.* 55 (1), 1–31.
- Yunker, M.B., Macdonald, R.W., Vingarzan, R., Mitchell, R.H., Goyette, D., Sylvestre, S., 2002b. PAHs in the Fraser River basin: a critical appraisal of PAH ratios as indicators of PAH source and composition. *Org. Geochem.* 33 (4), 489–515.
- Zakaria, M.P., Horinouchi, A.I., Tsutsumi, S., Takada, H., Tanabe, S., Ismail, A., 2000. Oil pollution in the straits of Malacca, Malaysia: application of molecular markers for source identification. *Environmental Science & Technology* 34 (7), 1189–1196.
- Zakaria, M.P., Okuda, T., Takada, H., 2001. Polycyclic aromatic hydrocarbon (PAHs) and hopanes in stranded tar balls on the coasts of Peninsular Malaysia: applications of biomarkers for identifying sources of oil pollution. *Mar. Pollut. Bull.* 42 (12), 1357–1366.
- Zakaria, M.P., Takada, H., Tsutsumi, S., Ohno, K., Yamada, J., Kouno, E., Kumata, H., 2002. Distribution of polycyclic aromatic hydrocarbons (PAHs) in rivers and estuaries in Malaysia: a widespread input of petrogenic PAHs. *Environmental Science & Technology* 36 (9), 1907–1918.
- Zhang, J., Cai, L., Yuan, D., Chen, M., 2004. Distribution and sources of polynuclear aromatic hydrocarbons in Mangrove surficial sediments of Deep Bay, China. *Mar. Pollut. Bull.* 49 (5–6), 479–486.
- Zhao, Z., Zhang, L., Cai, Y., Chen, Y., 2014. Distribution of polycyclic aromatic hydrocarbon (PAH) residues in several tissues of edible fishes from the largest freshwater lake in China, Poyang Lake, and associated human health risk assessment. *Ecotoxicol. Environ. Saf.* 104, 323–331.